Tris$^+$/Na$^+$ Permeability Ratios of Nicotinic Acetylcholine Receptors Are Reduced by Mutations near the Intracellular End of the M2 Region

BRUCE N. COHEN, CESAR LABARCA, LINDA CZYZYK, NORMAN DAVIDSON, and HENRY A. LESTER

From the Division of Biology 156-29, California Institute of Technology, Pasadena, California 91125

ABSTRACT Tris$^+$/Na$^+$ permeability ratios were measured from shifts in the biionic reversal potentials of the macroscopic ACh-induced currents for 3 wild-type (WT), 1 hybrid, 2 subunit-deficient, and 25 mutant nicotinic receptors expressed in *Xenopus* oocytes. At two positions near the putative intracellular end of M2, 2' (αThr244, βGly255, γThr253, δSer258) and $-1'$, point mutations reduced the relative Tris$^+$ permeability of the mouse receptor as much as threefold. Comparable mutations at several other positions had no effects on relative Tris$^+$ permeability. Mutations in δ had a greater effect on relative Tris$^+$ permeability than did comparable mutations in γ; omission of the mouse δ subunit (δ_0 receptor) or replacement of mouse δ with *Xenopus* δ dramatically reduced relative Tris$^+$ permeability. The WT mouse muscle receptor ($\alpha\beta\gamma\delta$) had a higher relative permeability to Tris$^+$ than the wild-type *Torpedo* receptor. Analyses of the data show that (a) changes in the Tris$^+$/Na$^+$ permeability ratio produced by mutations correlate better with the hydrophobicity of the amino acid residues in M2 than with their volume; and (b) the mole-fraction dependence of the reversal potential in mixed Na$^+$/Tris$^+$ solutions is approximately consistent with the Goldman-Hodgkin-Katz voltage equation. The results suggest that the main ion selectivity filter for large monovalent cations in the ACh receptor channel is the region delimited by positions $-1'$ and 2' near the intracellular end of the M2 helix.

INTRODUCTION

Previous work (Dwyer, Adams, and Hille, 1980) suggests that the nicotinic acetylcholine receptor channel (nAChR) acts like a simple molecular sieve, selectively excluding cations on the basis of their size. The nAChR is permeable to a wide variety of organic and inorganic cations, as well as to some small uncharged molecules (Maeno, Edwards, and Anraku, 1977; Huang, Catterall, and Ehrenstein, 1978; Adams, Dwyer, and Hille, 1980; Dwyer et al., 1980). The selectivity for monovalent metal cations is

weak (Adams et al., 1980). The permeability of monovalent organic cations decreases monotonically with the size of the cation. Permeability approaches zero for cation dimensions near 6.5 Å × 6.5 Å (Dwyer et al., 1980). This observation suggests that the selectivity of the nAChR for monovalent organic cations is determined by a narrow region of the pore with a cross-section of ~6.5 Å × 6.5 Å (Dwyer et al., 1980). Streaming potential measurements indicate that the longitudinal dimension of the

MOUSE

	-1	0		1	2	3	4	5	6	7	8	9	10	11	12	13	14	15	16	17	18	19		20	21
α	E	K		M	T	L	S	I	S	V	L	L	S	L	T	V	F	L	L	V	I	V		E	L
β	E	K		M	G	L	S	I	F	A	L	L	T	L	T	V	F	L	L	L	L	A		D	K
γ	Q	K		C	T	V	A	T	N	V	L	L	A	Q	T	V	F	L	F	L	V	A		K	K
δ	E	K		T	S	V	A	I	S	V	L	L	A	Q	S	V	F	L	L	L	I	S		K	R
ε	Q	K		C	T	V	S	I	N	V	L	L	A	Q	T	V	F	L	F	L	I	A		Q	K

TORPEDO

	-1	0		1	2	3	4	5	6	7	8	9	10	11	12	13	14	15	16	17	18	19		20	21
α	E	K		M	T	L	S	I	S	V	L	L	S	L	T	V	F	L	L	V	I	V		E	L
β	E	K		M	S	L	S	I	S	A	L	L	A	V	T	V	F	L	L	L	L	A		D	K
γ	Q	K		C	T	L	S	I	S	V	L	L	A	Q	T	I	F	L	F	L	I	A		Q	K
δ	E	S		M	S	T	A	I	S	V	L	L	A	Q	A	V	F	L	L	L	T	S		Q	R

XENOPUS

	-1	0		1	2	3	4	5	6	7	8	9	10	11	12	13	14	15	16	17	18	19		20	21
δ	E	K		M	T	L	A	I	S	V	L	L	A	Q	S	V	F	L	L	L	I	S		Q	R

FIGURE 1. Aligned amino acid sequences for the mouse (LaPolla, Mixter-Mayne, and David-son, 1985; Isenberg, Mudd, Shah, and Merlie, 1986; Yu, LaPolla, and Davidson, 1986; Gardner, 1990), Torpedo (Noda, Takahashi, Tanabe, Toyosato, Furutani, Hirose, Asai, Inayama, Miyata, and Numa, 1982; Claudio, Ballivet, Patrick, and Heinemann, 1983; Noda, Takahashi, Tanabe, Toyosato, Kikyotani, Hirose, Asai, Takashima, Inayama, Miyata, and Numa, 1983), and Xenopus M2 regions (Baldwin, Yoshihara, Blackmer, Kinter, and Burden, 1988). Amino acids are given by the single letter code. The NH₂ -terminus of M2 was labeled position 1' (Charnet et al., 1990) and corresponds to αMet243, βMet254, γCys252, and δThr257 in terms of the total sequence numbers. Subunits are indicated at left and position number in M2 is indicated above the sequence.

narrowest region of the nAChR is 3–6 Å (Dani, 1989), suggesting that the ion selectivity filter of the nAChR is confined to a fairly small region of the channel pore. This paper localizes the region responsible for $Na^+/Tris^+$ selectivity.

The M2 region of the nAChR is thought to line the channel pore (see Stroud, McCarthy, and Shuster, 1990; Lester, 1992) and point mutations suggest that the

narrowest portion of the pore is within the amino (NH_2)-terminal half of M2 (Imoto, Busch, Sakmann, Mishina, Konno, Nakai, Bujo, Mori, Fukuda, and Numa, 1988; Leonard, Labarca, Charnet, Davidson, and Lester, 1988; Charnet, Labarca, Leonard, Vogelaar, Czyzyk, Gouin, Davidson, and Lester, 1990; Konno, Busch, von Kitzing, Imoto, Wang, Nakai, Mishina, Numa, and Sakmann, 1991; Villarroel, Herlitze, Koenen, and Sakmann, 1991), which is between positions $-1'$ and $6'$ according to our numbering system (see Fig. 1). There might also be an important ion-binding site near the carboxy (COOH) terminus of M2 at position $14'$ (Eisenman, Villarroel, Montal, and Alvarez, 1990).

Reversal potential measurements provide the most appropriate and sensitive technique for assessing small changes in pore structure; we expected that such changes might dramatically alter the permeability of large cations such as $Tris^+$. To test the hypothesis that the ion selectivity of the nAChR is determined by this narrow region of the pore and to localize the selectivity filter more precisely, we examined the effect of point mutations in M2 on the $Tris^+/Na^+$ permeability ratio (P_{Tris}/P_{Na}) of the mouse nAChR. Wild-type (WT) and mutated nAChR's were expressed in *Xenopus* oocytes (Mishina, Kurosaki, Tobimatsu, Morimoto, Noda, Yamamoto, Terao, Lindstrom, Takahashi, Kuno, and Numa, 1984; White, Mixter-Mayne, Lester, and Davidson, 1985) and P_{Tris}/P_{Na} was determined electrophysiologically from the shift in the biionic reversal potential of the macroscopic ACh-induced current (Dwyer et al., 1980).

The results suggest that the main ion selectivity filter of the nAChR for large monovalent cations is localized to a region delimited by positions $-1'$ and $2'$ near the NH_2-terminus of M2, and that the hydrophobicity of the residues in this region is a more important determinant of ion selectivity than the volume of the residues. The results also show that nAChR's formed without the δ subunit (δ_0 receptors) have a much lower relative permeability to $Tris^+$ than the WT mouse and γ_0 receptors.

A preliminary report of these results has appeared in abstract form (Cohen, Labarca, Davidson, and Lester, 1991).

METHODS

Source of Wild-Type nAChR's

Sources of the cDNA clones for the mouse and *Torpedo* α, β, γ, and δ subunits have been described previously (White et al., 1985; Yoshii, Yu, Mixter-Mayne, Davidson, and Lester, 1987). The mouse subunits were cloned from the BC3H-1 cell line. The mouse ϵ subunit was generously provided by Dr. P. Gardner, Dartmouth Medical School, and the *Xenopus* δ subunit by Dr. S. Burden, Massachusetts Institute of Technology.

Point Mutations

Point mutations are indicated in the text by subscripts of the mutated subunits containing first, the single letter code of the original amino acid; second, the number of the position in M2; and third, the single letter code of the replacement amino acid. For example, $\delta_{S2'F}$ represents a δ subunit mutated at position $2'$ so the original serine is replaced by phenylalanine. Mutations and mRNA synthesis were carried out as previously described (Leonard et al., 1988; Charnet et al., 1990).

Oocyte Expression

Oocytes were injected with 2–19 ng of mRNA per nAChR subunit, generally in the ratio 2:1:1:1 (α:β:γ:δ), and incubated in a modified Barth's solution (96 mM NaCl, 2 mM KCl, 1.8 mM CaCl$_2$, 1 mM MgCl$_2$, 2.5 mM sodium pyruvate, 0.1 mg/ml gentamicin sulfate, and 5 mM HEPES, pH 7.4) for 2–10 d before recording. Gentamicin was removed from the incubation media in later experiments because it inhibits WT nAChR expression (Okamoto and Sumikawa, 1991).

Voltage Clamp of Oocytes

The oocytes were voltage clamped with two microelectrodes using an Axoclamp 2A voltage clamp circuit (Axon Instruments, Inc., Foster City, CA). Both microelectrodes were filled with 3 M KCl and had resistances of 0.5–1.5 MΩ. Membrane voltage was recorded differentially using a 1 M KCl salt bridge as a bath reference electrode. The current ground was either an Ag-AgCl pellet or another 1 M KCl salt bridge. The highest possible gain of the voltage clamp ($\sim$ 10,000) was used to minimize errors in the holding potential. All recordings were made at room temperature (23–25°C) with continuous saline superfusion.

Generation of Macroscopic Current–Voltage Relations

Current–voltage (I-V) relations for the whole oocyte were generated by ramping the potential within a 60–120-mV range around the expected reversal potential of the current over a period of 0.9 s. An MS-DOS computer equipped with pCLAMP V5.5 software (Axon Systems, Foster City, CA) controlled the command potential and recorded the voltage clamp currents. Current signals were analog filtered with an eight-pole, low-pass Bessel filter (Frequency Devices Inc., Haverhill, MA) at 100–250 Hz and were digitally sampled at a frequency 4–10 times higher than the corner frequency (f_c) of the filter. We obtained the mean I-V relation for the ACh-induced current by ramping the voltage three times in the presence and absence of bath-applied ACh (10^{-7}–10^{-2} M) and digitally subtracting the mean background current from the mean current in ACh. The biionic reversal potential for the agonist-induced current (V_r) was read directly from the ACh-induced I-V relation or by fitting a straight line to the portion of the curve surrounding V_r. We found little or no response to ACh in noninjected oocytes even at the highest concentration used (10 mM ACh).

Measurement of Permeability Ratios

Permeability ratios for the nAChR were determined from shifts in V_r (Dwyer et al., 1980). V_r was measured for each oocyte first in a NaCl solution containing 98 mM NaCl, 1 mM MgCl$_2$, 2 mM NaOH, and 5 mM HEPES (pH 7.4–7.5), followed by a measurement in a Tris·HCl solution containing 114 mM Tris·OH, 1 mM MgCl$_2$, 5 mM buffer (HEPES or ACES, depending on the pH required), and enough HCl to bring the solution to pH 6.3 or 7.4. Ca^{2+} was omitted from the bathing solutions to suppress the endogenous Ca^{2+}-activated Cl$^-$ current (Miledi, 1982; Barish, 1983). MgCl$_2$ (1 mM) was included because we found large background conductances in the absence of external divalents. In some experiments we added 75 μM niflumic or flufenamic acid and 1–10 μM atropine sulfate to suppress the background Cl$^-$ conductance (White and Aylwin, 1990) and residual muscarinic responses (Dascal, 1987). The junction potential of the 1 M KCl salt bridge in different cation solutions was measured with a ceramic frit reference electrode (Beckman Instruments, Inc., Fullerton, CA). Shifts in V_r were corrected for changes in this potential. We omitted the external Mg^{2+} concentration in our calculation of permeability ratios.

Single-Channel Recordings

Single ACh-activated channels for the mouse WT ($\alpha\beta\gamma\delta$) and $\alpha\beta\gamma\delta_{S2'F}$ mutant were recorded in outside-out patches in a symmetrical KCl solution (100 mM KCl, 2 mM MgCl$_2$, 10 mM EGTA, 5 mM KOH, and 10 mM HEPES, pH 7.4) as previously described (Leonard et al., 1988). We measured single-channel conductance in one of two ways: (a) by ramping the voltage and fitting a straight line to the channel openings by eye, or (b) by compiling all-points, amplitude histograms of the current at one or more potentials and fitting the sum of two or more Gaussian curves to the histogram data using pCLAMP. Estimates of the slope and chord conductance were consistent with each other, as were estimates of the slope conductance using either of the two methods outlined above. Data for the histograms were filtered at 2 kHz with an eight-pole, low-pass Bessel filter and sampled at 8 kHz. Recordings were made at either 13 or 23°C. ACh concentrations were 100 μM for $\alpha\beta\gamma\delta_{S2'F}$ and 0.5, 1, or 100 μM for $\alpha\beta\gamma\delta$. We found no differences in the conductance levels of $\alpha\beta\gamma\delta$ at different agonist concentrations. There were not enough openings in the $\alpha\beta\gamma\delta_{S2'F}$ patches to compare the kinetics of the $\alpha\beta\gamma\delta$ and $\alpha\beta\gamma\delta_{S2'F}$ channels.

Statistical Analysis

We used the Tukey HSD test (Zar, 1984), as implemented in SYSTAT V.4, (SYSTAT Inc., Evanston, IL), to detect significant differences between multisample means. All the data on the mean relative permeabilities of the receptors to Tris$^+$ were included in a single test of significance, except for the data on the effects of varying the concentration of the δ subunit, which were tested separately.

RESULTS

Point mutations were made at positions $-1'$, $2'$, $6'$, $10'$, and $14'$ because previous experiments (Giraudat, Dennis, Heidmann, Chang, and Changeux, 1986; Oberthür, Muhn, Baumann, Lottspeich, Wittmann-Liebold, and Hucho, 1986; Imoto et al., 1988; Leonard et al., 1988; Charnet et al., 1990; Revah, Galzi, Giraudat, Haumont, Lederer, and Changeux, 1990; Konno et al., 1991; Villarroel et al., 1991) and an energy-minimized model of M2 (Oiki, Madison, and Montal, 1990) suggested that these residues face the pore. In addition to these mutations, a single mutation was made at a position not thought to face the pore (position $12'$).

Mutations Had Little Effect on Reversal Potentials in NaCl

Changes in the amino acid composition of the nAChR had little effect on V_r in the standard NaCl solution, V_r(Na). We measured mean V_r(Na) for 34 different nAChR receptor types expressed in *Xenopus* oocytes. The most reliable estimate of mean V_r(Na) was the value for the WT mouse receptor ($\alpha\beta\gamma\delta$). The $\alpha\beta\gamma\delta$ receptor had the highest level of expression and largest sample size. Mean V_r(Na) for $\alpha\beta\gamma\delta$ was -7 ± 4 mV (mean $\pm$ SD, $n = 142$), near previously reported reversal potentials for WT nAChR's expressed in oocytes and bathed in similar solutions (Sakmann, Methfessel, Mishina, Takahashi, Takai, Kurasaki, Fukuda, and Numa, 1985; Yoshii et al., 1987; Kullberg, Owens, Camacho, Mandel, and Brehm, 1990). Mean V_r(Na) for the other 33 receptor types ranged from -2 to -11 mV ($n = 3$–53). Two receptors displayed a mean V_r(Na) that was marginally different ($0.04 \leq P \leq 0.05$) from $\alpha\beta\gamma\delta$: $\alpha\beta\delta\epsilon_5$ and

αβγδ$_x$. Mean V_r(Na) was −2 ± 2 mV (n = 4) for αβδε$_5$, the receptor with five times the concentration of the ε subunit substituted for γ, and −2 ± 4 mV (n = 23) for αβγδ$_x$, the mouse-*Xenopus* hybrid with mouse α, β, and γ, and *Xenopus* δ. We did not explore these results in greater detail. The overall mean V_r(Na), excluding these two receptor types, was −5 ± 4 mV (n = 634). Changes in the external pH (5.7–7.4) and the concentration of ACh (1–10 μM), or the addition of 75 μM niflumic acid, 100 μM atropine, 1 mM Mg^{2+}, or 3 mM Ba^{2+} to the bath did not affect V_r(Na). The absence of an effect of external pH on V_r(Na) was consistent with previous data (Ritchie and Fambrough, 1975; Trautmann and Zilber-Gachelin, 1976).
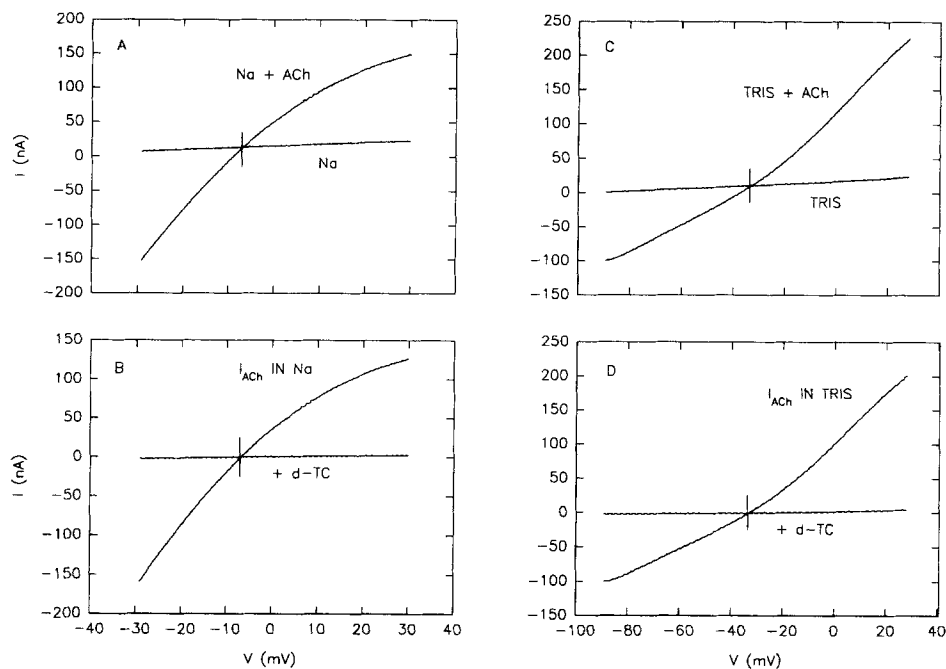
FIGURE 2.   *I-V* relations for an oocyte injected with mRNA for the WT mouse nAChR (αβγδ) and voltage-clamped with two microelectrodes. Vertical lines indicate the reversal potential (V_r) of the ACh-induced current (I_{ACh}). (*A*) *I-V* relations in NaCl with and without ACh. (*B*) I_{ACh} in NaCl with and without 5 μM d-TC present. (*C*) *I-V* relations in Tris·HCl with and without ACh. (*D*) I_{ACh} in Tris·HCl with and without 10 μM d-TC.

Wild-Type Mouse and Torpedo Receptors Have Different Tris[+] Permeabilities

Fig. 2 shows an example of macroscopic *I-V* relations for the mouse αβγδ in NaCl and in Tris·HCl. The curves in Fig. 2*A* were generated by ramping the potential from −30 to +30 mV in NaCl with and without 1 μM ACh present, and the curves in Fig. 2*C* were generated by ramping from −90 to +30 mV in Tris·HCl with and without 5 μM ACh present. Fig. 2, *B* and *D*, shows *I-V* relations for the ACh-induced current (I_{ACh}). I_{ACh} reversed at −7 mV in NaCl and at −34 mV in Tris·HCl, and also showed the rectification (Fig. 2*B*) typical of a muscle nAChR in NaCl (Mishina et al.,

1985; Yoshii et al., 1987). I_{ACh} was almost completely blocked by 5 μM d-tubocurarine (d-TC) in NaCl (Fig. 2 *B*) and 10 μM d-TC in Tris·HCl (Fig. 2 *D*).

The ratio of the $Tris^+$ to Na^+ permeability, P_{Tris}/P_{Na}, is related to the difference between the reversal potential in $Tris^+$ and Na^+, $[V_r(Tris) - V_r(Na)]$, by the following equation:

$$\frac{P_{Tris}}{P_{Na}} = \frac{[Na^+]}{[Tris^+]} 10^{[V_r(Tris) - V_r(Na)]/59 \text{ mV}}$$

where 59 mV is $2.3RT/F$ at 23°C, $[Tris^+]$ is the external $Tris^+$ concentration, and $[Na^+]$ is the external Na^+ concentration. For the experiment of Fig. 2, V_r shifted −27 mV after 100 mM Na^+ was replaced with 98 mM $Tris^+$. Thus, P_{Tris}/P_{Na} was 0.36, assuming that pK_a (Tris) = 8.2 at 23°C (Good, Winget, Winter, Connolly, Izawa, and Singh, 1966).

Mean P_{Tris}/P_{Na} for the mouse αβγδ was about twice as large as that for the *Torpedo* WT nAChR, $(αβγδ)_T$. Mean $[V_r(Tris) - V_r(Na)]$ was −27 ± 3 mV (*n* = 59) for αβγδ after 100 mM external Na^+ was replaced with 98 mM $Tris^+$, and −39 ± 5 mV (*n* = 4) for $(αβγδ)_T$. Mean P_{Tris}/P_{Na} was 0.36 ± 0.04 for αβγδ and 0.22 ± 0.05 for $(αβγδ)_T$.

Mean P_{Tris}/P_{Na} for $(αβγδ)_T$ was consistent with the previous estimate of 0.18 obtained from reconstituted *Torpedo* nAChR's in lipid bilayers (Oiki, Dahno, Madison, and Montal, 1988) and from frog nAChR's at the motor endplate (Dwyer et al., 1980). Mean P_{Tris}/P_{Na} for αβγδ was higher than these values, but it was close to the 0.30 obtained for frog nAChR's using internal cation concentrations measured by flame photometry (Fiekers and Henderson, 1982).

We had to use higher agonist concentrations to obtain responses from oocytes injected with $(αβγδ)_T$ than those injected with αβγδ. However, raising the ACh concentration for αβγδ to the same levels used for $(αβγδ)_T$, while adding 10 μM d-TC to avoid saturating the voltage clamp, did not affect V_r for the mouse nAChR in Tris·HCl (*n* = 10). Thus, the difference between P_{Tris}/P_{Na} for the mouse and *Torpedo* nAChR's was not an artifact of agonist concentration.

To control for the possibility that enough uncharged Tris crossed the oocyte membrane at pH 7.4 to raise the apparent P_{Tris}/P_{Na} for the mouse nAChR, we measured P_{Tris}/P_{Na} for the mouse αβγδ at pH 7.4 and 6.3. About 14% of the external Tris was uncharged at pH 7.4, and 1% at pH 6.3. Lowering the pH from 7.4 to 6.3 had no effect on P_{Tris}/P_{Na} (*n* = 8). Thus, the movement of uncharged Tris across the oocyte membrane at pH 7.4 was not sufficient to raise the apparent P_{Tris}/P_{Na} for the mouse nAChR.

Mutations Change the Permeability to Tris+

A number of the point mutations in M2 significantly altered the relative permeability of the mouse nAChR to $Tris^+$. 39 combinations of mouse muscle receptor mRNAs with point mutations were injected into oocytes. 25 of these mutants yielded currents sufficiently large for the measurement of the reversal potentials in $Tris^+$. For individual mutants in this group, mean $[V_r(Tris) - V_r(Na)]$ ranged from −26 to −59 mV, and mean P_{Tris}/P_{Na} ranged from 0.37 to 0.11.

Fig. 3 summarizes the relationship between the position of a mutation in M2 and its effect on the relative permeability of the channel to $Tris^+$, as measured by

$[V_r(\text{Tris}) - V_r(\text{Na})]$. More negative values of $[V_r(\text{Tris}) - V_r(\text{Na})]$ imply a smaller relative Tris$^+$ permeability. 13 of the 17 receptors with mutations at positions $-1'$ or $2'$ had a mean $[V_r(\text{Tris}) - V_r(\text{Na})]$ that was less than the WT mean minus 2 SD and had Tris$^+$/Na$^+$ permeability ratios that were significantly different from the WT (see below). For the seven receptors with mutations at positions $6'$, $10'$, $12'$, and $14'$, $[V_r(\text{Tris}) - V_r(\text{Na})]$ fell within 2 SD of the WT mean and Tris$^+$/Na$^+$ permeability ratios were not significantly different from the WT (see below). Mutations at positions $6'$ and $10'$ did not affect the relative permeability of the channel to Tris$^+$ even though previous data indicate that these two positions face the pore (Leonard et al., 1988; Charnet et al., 1990). $[V_r(\text{Tris}) - V_r(\text{Na})]$ for the single receptor we tested with
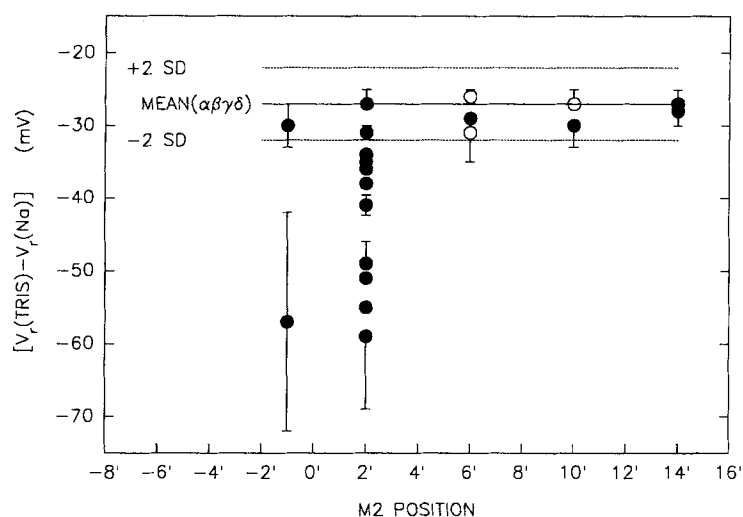
FIGURE 3.   Relationship between the position of mutations in M2 and $[V_r(\text{Tris}) - V_r(\text{Na})]$, the difference between the reversal potential of I_{ACh} in Tris·HCl and NaCl. Points represent mean $[V_r(\text{Tris}) - V_r(\text{Na})]$ for 25 mutant receptors of $\alpha\beta\gamma\delta$ (17 mutants at position $2'$; some individual points lying between -20 and -40 mV are obscured by others). Error bars show standard deviation (SD) of mean. Mutants that affect QX-222 binding (Leonard et al., 1988; Charnet et al., 1990) are shown as hollow circles. Solid horizontal line denotes $[V_r(\text{Tris}) - V_r(\text{Na})]$ for $\alpha\beta\gamma\delta$ and dotted lines give $\pm$ 2 SD.

mutations at both positions $10'$ and $12'$ ($\alpha_{S10'A}\beta\gamma_{T12'A}\delta$) also fell within 2 SD of the WT mean (plotted as a filled circle at position 10 in Fig. 3).

Fig. 4 A shows ACh-induced I-V relations in NaCl and in Tris·HCl for a position $2'$ mutant with one of the lowest Tris$^+$/Na$^+$ permeability ratios, $\alpha\beta\gamma\delta_{S2'F}$. The I-V relations in NaCl were generated by applying 50 μM ACh and ramping the potential from -30 to $+30$ mV, and in Tris·HCl by applying 100 μM ACh and ramping the potential from -120 to 0 mV. I_{ACh} reversed at $+1$ mV in NaCl and at -49 mV in Tris·HCl. Thus, $[V_r(\text{Tris}) - V_r(\text{Na})]$ was -50 mV for this oocyte; $P_{\text{Tris}}/P_{\text{Na}}$ was 0.14.

The $\alpha\beta\gamma\delta_{S2'F}$ mutation also slightly altered the rectification of I_{ACh} in NaCl (Fig. 4 B). Fig. 4 B shows whole-oocyte I-V relations taken from one oocyte injected with $\alpha\beta\gamma\delta$ and from another oocyte injected with $\alpha\beta\gamma\delta_{S2'F}$ at agonist concentrations where

desensitization occurred too slowly to distort the *I-V* relations during ramps (3 μM ACh for αβγδ and 10 μM ACh for αβγδ$_{S2'F}$). The *I-V* relations were normalized by translating the αβγδ curve along the voltage axis to match the reversal potential of the αβγδ$_{S2'F}$ curve and then dividing the αβγδ current by a scaling factor to equate the αβγδ and αβγδ$_{S2'F}$ currents at −117 mV. In the resulting curves in Fig. 4 *B*, the ACh-induced current for αβγδ$_{S2'F}$ rectified more strongly inwardly than did the current for the WT.
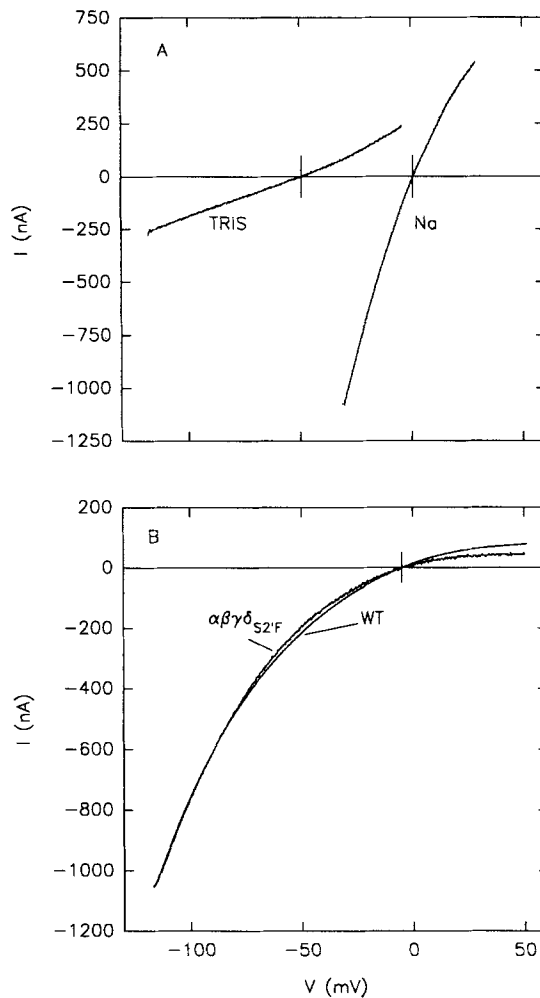
FIGURE 4. ACh-induced *I-V* relations for αβγδ$_{S2F}$ and αβγδ (WT). Horizontal line indicates *I* = 0 nA. (*A*) ACh-induced *I-V* relations in NaCl and in Tris·HCl from an oocyte injected with αβγδ$_{S2'F}$. (*B*) ACh-induced *I-V* relations in NaCl for αβγδ$_{S2'F}$ and αβγδ generated by ramping the command voltage from −120 to +50 mV and applying 3 μM ACh to the αβγδ-injected oocyte and 10 μM ACh to the αβγδ$_{S2'F}$-injected oocyte. V_r(Na) was originally −6 mV for αβγδ and −5 mV for αβγδ$_{S2'F}$. The magnitude of I_{ACh} for the WT was 5.27 times greater than that for αβγδ$_{S2'F}$ at −117 mV. We shifted the αβγδ *I-V* relation +1 mV along the voltage axis and divided the current by a factor of 5.3 to obtain the *I-V* relation for αβγδ shown in the figure.

We used P_{Tris}/P_{Na}, rather than [V_r(Tris) − V_r(Na)], to determine which mutant receptors were significantly different from the WT. The permeability ratio contains the same information as the difference in the reversal potential. However, the Tukey HSD test assumes homogeneous sample variance and we found that transforming [V_r(Tris) − V_r(Na)] to P_{Tris}/P_{Na} reduced the heterogeneity of the sample variance.

Only receptors with mutations at positions $-1'$ or $2'$ had relative permeabilities to Tris$^+$ that were significantly different ($P < 0.01$) from the WT. Table I gives mean $[V_r(\text{Tris}) - V_r(\text{Na})]$ and $P_{\text{Tris}}/P_{\text{Na}}$ for the 13 mutant receptors that were significantly different. Mean $P_{\text{Tris}}/P_{\text{Na}}$ in Table I ranged from 0.11 to 0.27 and was 35–60% less than the WT mean ($P_{\text{Tris}}/P_{\text{Na}} = 0.36$). The five mutant receptors with the lowest relative permeabilities to Tris$^+$ were $\alpha\beta\gamma\delta_{S2'T}$, $\alpha\beta\gamma\delta_{E-1'Q}$, $\alpha_{T2'A}\beta\gamma\delta_{S2'A}$, $\alpha\beta\gamma\delta_{S2'F}$, and $\alpha_{T2'A}\beta_{G2'S}\gamma\delta_{S2'A}$, and they were not significantly different from each other. None of the mutations significantly increased $P_{\text{Tris}}/P_{\text{Na}}$.

The following 12 mutant receptors had relative Tris$^+$ permeabilities that were not significantly different from the WT: $\alpha\beta\gamma_{Q-1'E}\delta$, $\alpha\beta_{G2'S}\gamma\delta$, $\alpha\beta\gamma_{T2'S}\delta$, $\alpha\beta\gamma_{T2'A}\delta$, $\alpha_{S6'A}\beta\gamma\delta_{S6'A}$, $\alpha\beta_{F6'S}\gamma\delta$, $\alpha\beta\gamma\delta_{S6'F}$, $\alpha_{S10'A}\beta_{T10'A}\gamma\delta$, $\alpha_{S10'A}\beta\gamma_{T12'A}\delta$, $\alpha\beta_{F14'Y}\gamma\delta$, $\alpha\beta\gamma_{F14'Y}\delta$, and $\alpha\beta\gamma_{F14'S}\delta$. Mean $P_{\text{Tris}}/P_{\text{Na}}$ for these mutants ranged from 0.30 to 0.37 ($n = 7$–18). Note that the position $2'$ mutants $\alpha\beta\gamma\delta_{S2'F}$ and $\alpha_{T2'A}\beta\gamma\delta_{S2'A}$ had significantly lower relative Tris$^+$

TABLE I

Mutations That Affect $P_{\text{Tris}}/P_{\text{Na}}$ Significantly

Mutant	$V_r(\text{Tris}) - V_r(\text{Na})$	$P_{\text{Tris}}/P_{\text{Na}}$	n
	mV		
$\alpha\beta\gamma\delta$ (WT)	-27 ± 3*	0.36 ± 0.04*	59
$\alpha\beta\gamma\delta_{S2'T}$	-59 ± 11	0.11 ± 0.06	19
$\alpha\beta\gamma\delta_{E-1'Q}$	-57 ± 17	0.13 ± 0.08	7
$\alpha_{T2'A}\beta\gamma\delta_{S2'A}$	-55 ± 9	0.13 ± 0.04	9
$\alpha\beta\gamma\delta_{S2'F}$	-50 ± 3	0.15 ± 0.02	9
$\alpha_{T2'A}\beta_{G2'S}\gamma\delta_{S2'A}$	-49 ± 3	0.15 ± 0.02	13
$\alpha\beta\gamma_{T2'Y}\delta$	-41 ± 2	0.21 ± 0.01	11
$\alpha\beta\gamma_{T2'A}\delta_{S2'A}$	-38 ± 7	0.24 ± 0.06	5
$\alpha\beta\gamma_{T2'F}\delta$	-36 ± 1	0.25 ± 0.01	10
$\alpha\beta\gamma_{T2'L}\delta$	-36 ± 4	0.26 ± 0.04	12
$\alpha_{T2'A}\beta_{G2'S}\gamma_{T2'A}\delta$	-35 ± 2	0.26 ± 0.02	5
$\alpha_{T2'A}\beta\gamma\delta$	-34 ± 1	0.27 ± 0.01	11
$\alpha\beta\gamma\delta_{S2'A}$	-34 ± 4	0.27 ± 0.04	15
$\alpha_{T2'A}\beta\gamma_{T2'A}\delta$	-34 ± 5	0.27 ± 0.05	5

*Mean ± SD.

permeabilities than the WT (Table I); but similar mutations at other positions, such as $\alpha\beta\gamma\delta_{S6'F}$, $\alpha\beta_{F6'S}\gamma\delta$, $\alpha\beta\gamma_{F14'S}\delta$, $\alpha_{S6'A}\beta\gamma\delta_{S6'A}$, and $\alpha_{S10'A}\beta_{T10'A}\gamma\delta$, did not affect relative Tris$^+$ permeability.

The data given above suggest that positions $-1'$ and $2'$ are major loci of Tris$^+$ selectivity in the WT mouse receptor. However, the difference between the relative permeabilities of the mouse and *Torpedo* WTs to Tris$^+$ was not due to differences in the residues at positions $-1'$ and $2'$. The mouse $\alpha\beta\gamma\delta$ receptor has the same amino acids at positions $-1'$ and $2'$ as $(\alpha\beta\gamma\delta)_T$ except that mouse has a glycine (G) at position $2'$ in β and *Torpedo* has a serine (S) (see Fig. 1). Thus, the mouse mutant, $\alpha\beta_{G2'S}\gamma\delta$, was identical to $(\alpha\beta\gamma\delta)_T$ at positions $-1'$ and $2'$ (see Fig. 1). Nevertheless, it had nearly the same mean relative permeability to Tris$^+$ ($P_{\text{Tris}}/P_{\text{Na}} = 0.35 \pm 0.02$) as $\alpha\beta\gamma\delta$ rather than $(\alpha\beta\gamma\delta)_T$. Thus, changing $\alpha\beta\gamma\delta$ to match $(\alpha\beta\gamma\delta)_T$ at positions $-1'$ and $2'$ did not make the Tris$^+$/Na$^+$ permeability ratio of mouse and *Torpedo* nAChR's

equal. It seems that there are additional sites on the receptor, distinct from positions −1′ and 2′, that are important for Tris⁺ selectivity.

Tris⁺ Permeability Correlates with Side-Chain Hydrophobicity Better Than with Volume

To find out how physical changes in the pore wall affected Tris⁺ selectivity, we examined the correlation between the sum of the volumes (ΣV) or relative hydrophobicities ($\Sigma \Delta F_{AA}$) of the amino acids at position 2′, and $[V_r(\text{Tris}) - V_r(\text{Na})]\ P_{\text{Tris}}/P_{\text{Na}}$ for $\alpha\beta\gamma\delta$ and 15 position 2′ mutants. ΣV and $\Sigma \Delta F_{AA}$ were computed from previously published estimates for the volumes (Creighton, 1984) and relative hydrophobicities (Guy, 1985) of the amino acid side-chains. The α subunit was counted twice (we assumed a subunit stoichiometry of $\alpha{:}\beta{:}\gamma{:}\delta = 2{:}1{:}1{:}1$). The relative hydrophobicity of an amino acid was defined as the mean partition energy (ΔF_{AA}) required to transfer the amino acid from water to an organic solvent minus the energy required to transfer glycine (Guy, 1985). Thus, more hydrophobic residues are denoted by a more negative ΔF_{AA}. $\Sigma \Delta F_{AA}$ ranged from −0.62 kcal/mol ($\alpha\beta\gamma_{T2's}\delta$) to −2.67 kcal/mol ($\alpha\beta\gamma_{T2'F}\delta$), and ΣV from 416 Å^3 ($\alpha_{T2'A}\beta\gamma_{T2'A}\delta$) to 598 Å^3 ($\alpha\beta\gamma\delta_{S2'F}$).

The correlation between $P_{\text{Tris}}/P_{\text{Na}}$ and $\Sigma \Delta F_{AA}$ for the WT and the 15 receptors with mutations at position 2′ is shown in Fig. 5 *A*. The regression line in Fig. 5 *A* was fit to the raw data rather than to mean values of $P_{\text{Tris}}/P_{\text{Na}}$. The slope of the regression line was 0.074 ± 0.008 mol/kcal ($\pm$ standard error of estimate, SEE) and the intercept on the permeability axis (corresponding to a receptor with glycines in all the subunits at position 2′) was 0.37 ± 0.01.

Changes in the total relative hydrophobicity at position 2′ were a better overall predictor of the Tris⁺/Na⁺ permeability ratios than were changes in the total volume. The Pearson correlation coefficient (R) was 0.52 for $P_{\text{Tris}}/P_{\text{Na}}$ versus $\Sigma \Delta F_{AA}$, 0.41 for $[V_r(\text{Tris}) - V_r(\text{Na})]$ versus $\Sigma \Delta F_{AA}$, 0.18 for $P_{\text{Tris}}/P_{\text{Na}}$ versus ΣV, and 0.17 for $[V_r(\text{Tris}) - V_r(\text{Na})]$ versus ΣV ($n = 218$ oocytes). All four correlation coefficients were significant ($P < 0.01$), but $[V_r(\text{Tris}) - V_r(\text{Na})]$ and $P_{\text{Tris}}/P_{\text{Na}}$ were more strongly correlated with $\Sigma \Delta F_{AA}$ than with ΣV. $\Sigma \Delta F_{AA}$ accounted for 27% of the total variance of $P_{\text{Tris}}/P_{\text{Na}}$, while ΣV accounted for only 3% of the variance. Multivariate regression using both $\Sigma \Delta F_{AA}$ and ΣV did not significantly improve the predictive power of $\Sigma \Delta F_{AA}$ alone.

$P_{\text{Tris}}/P_{\text{Na}}$ and $[V_r(\text{Tris}) - V_r(\text{Na})]$ were more strongly correlated with $\Sigma \Delta F_{AA}$ if we included only mutations that did not increase the total volume of the side-chains at position 2′ (Fig. 5 *B*). ΣV for these mutants was between 84 and 100% of the WT value ($\Sigma V_{WT} = 497$ Å^3). R was 0.77 for $P_{\text{Tris}}/P_{\text{Na}}$ versus $\Sigma \Delta F_{AA}$, and 0.75 for $[V_r(\text{Tris}) - V_r(\text{Na})]$ versus $\Sigma \Delta F_{AA}$ ($n = 131$). The regression line fit to the raw data had a slope of 0.16 ± 0.01 mol/kcal and an intercept of 0.479 ± 0.01. $\Sigma \Delta F_{AA}$ accounted for 59% of the variance of $P_{\text{Tris}}/P_{\text{Na}}$ and 56% of the variance of $[V_r(\text{Tris}) - V_r(\text{Na})]$.

Mutations at Position 2′ in δ Have a Greater Effect Than Those in γ

To determine whether equivalent changes in the volume and relative hydrophobicity (ΔF_{AA}) of the amino acid at position 2′ in γ and δ differentially affected the relative permeability of the channel to Tris⁺, we examined the relation between $[V_r(\text{Tris}) - V_r(\text{Na})]$ and the volume (Fig. 6 *A*) or relative hydrophobicity (Fig. 6 *B*) of

the residue at position 2' for the WT and a series of point mutations at position 2' in
γ or δ. The lines in Fig. 6, A and B, represent regression lines fit to the raw data for the
γ and δ mutants, excluding $\alpha\beta\gamma\delta_{S2'T}$. [$V_r$(Tris) − V_r(Na)] for the γ mutants changed by
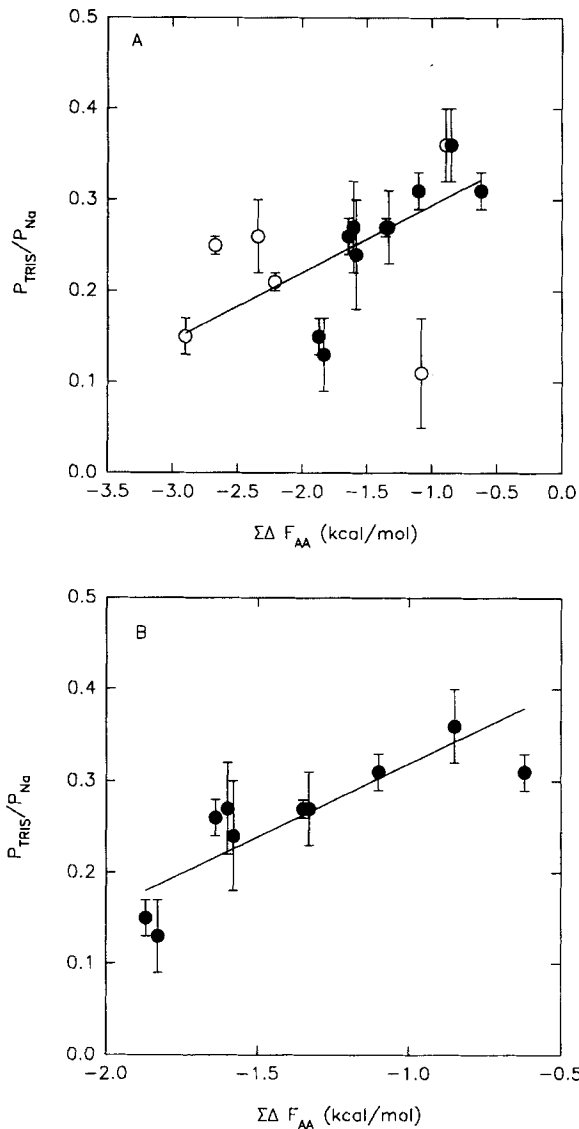-0.10 ± 0.01 mV/Å^3 as a function of side-chain volume and by 5.6 ± 0.4

FIGURE 5. Correlation be-
tween the Tris$^+$/Na$^+$ perme-
ability ratio (P_{Tris}/P_{Na}) and the
sum of the relative hydropho-
bicities ($\Sigma\Delta F_{AA}$) of the amino
acids at position 2'. The filled
circles represent the WT ($\alpha\beta\gamma\delta$)
and mutants for which the sum
of the amino acid side-chain
volumes at position 2' (ΣV)
was $\leq \Sigma V_{WT}$. The hollow circles
represent mutants with a $\Sigma V >$
ΣV_{WT}. Error bars are $\pm$ 1 SD.
Solid lines are regression lines
fit to the raw data. (A) P_{Tris}/P_{Na}
versus $\Sigma\Delta F_{AA}$ for the WT and all
the position 2' mutants. (B)
P_{Tris}/P_{Na} versus $\Sigma\Delta F_{AA}$ for the
WT and those position 2' mu-
tants with $\Sigma V \leq \Sigma V_{WT}$.

mV·kcal/mol as a function of side-chain hydrophobicity ($n = 119$ oocytes). On the
other hand, [V_r(Tris) − V_r(Na)] for the δ mutants changed by -0.21 ± 0.01 mV/Å^3 as
a function of side-chain volume and by 11.3 ± 0.5 mV·kcal/mol as a function of
side-chain hydrophobicity ($n = 83$). Thus, ignoring the anomalous behavior of

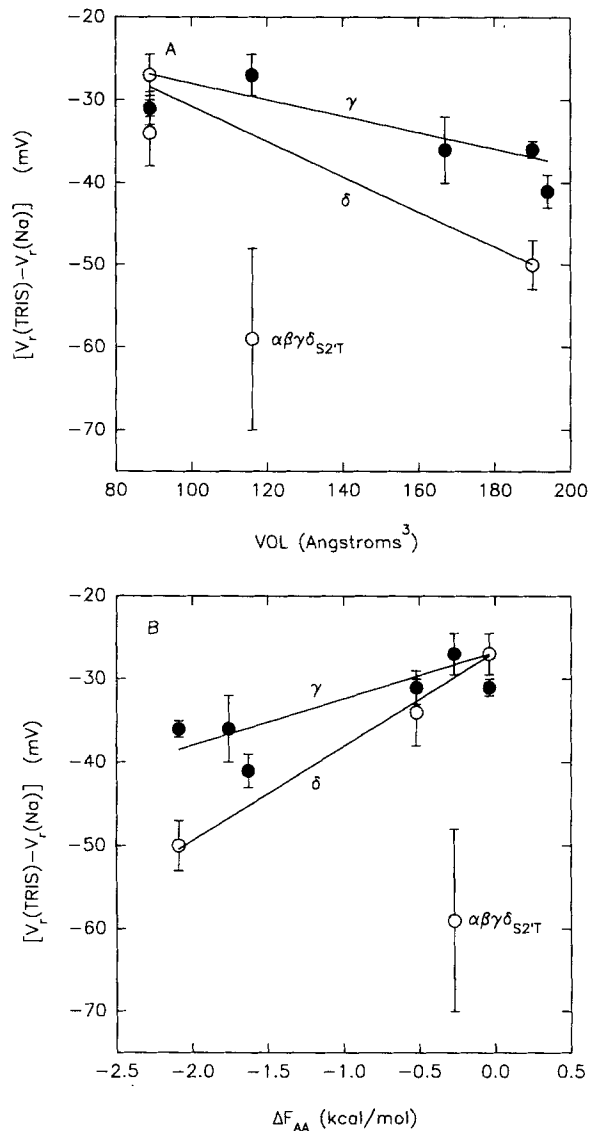FIGURE 6. Effects of mutations at position 2' in γ and δ on [V_r(Tris) − V_r(Na)]. Filled circles represent mean [V_r(Tris) − V_r(Na)] for the WT and γ mutants; hollow circles represent mean [V_r(Tris) − V_r(Na)] for the WT and δ mutants. Error bars are ± 1 SD. Lines denote linear regressions fit to the raw data excluding αβγδ$_{S2'T}$. (*A*) Mean [V_r(Tris) − V_r(Na)] versus the side-chain volume (VOL) of the amino acid at position 2'. (*B*) Mean [V_r(Tris) − V_r(Na)] versus the relative hydrophobicity of the amino acid at position 2' (ΔF_{AA}).

αβγδ$_{S2'T}$, mutations at position 2' in δ had a larger effect on [V_r(Tris) − V_r(Na)] than those in γ per unit change in volume or ΔF_{AA}. These results suggest that position 2' in δ plays a more important role in determining the selectivity of the nAChR to Tris$^+$ than does the corresponding site in γ.

Subunit Substitutions and Deletions Also Affect Tris$^+$ Permeability

We obtained ACh responses from oocytes injected with mouse αβγ (δ$_o$) or αβδ (γ$_o$) alone (White, 1987; Kullberg et al., 1990; Lo, Pinkham, and Stevens, 1990; Charnet, Labarca, and Lester, 1992), with ε instead of γ, or with a five times higher

concentration of ϵ (ϵ_5) instead of γ. The $\alpha\beta\gamma$, $\alpha\beta\delta$, $\alpha\beta\delta\epsilon$, and $\alpha\beta\delta\epsilon_5$ receptors gave much smaller responses to ACh than did $\alpha\beta\gamma\delta$ and required longer incubation periods for expression.

Table II gives mean $[V_r(\text{Tris}) - V_r(\text{Na})]$ and $P_{\text{Tris}}/P_{\text{Na}}$ for these receptors. The mouse δ_0 receptor and the mouse-*Xenopus* hybrid ($\alpha\beta\gamma\delta_X$) were practically impermeable to Tris$^+$; they displayed the lowest Tris$^+$/Na$^+$ permeability ratios of any receptor we tested ($P_{\text{Tris}}/P_{\text{Na}} \leq 0.06$). Fig. 7 A shows examples of ACh-induced I-V relations in NaCl and Tris·HCl from an oocyte injected with $\alpha\beta\gamma$ and incubated for 7 d. I_{ACh} reversed at -5 mV in NaCl and at -78 mV in Tris·HCl. $P_{\text{Tris}}/P_{\text{Na}}$ was 0.06. The currents shown in this figure represent the largest ACh responses we observed for $\alpha\beta\gamma$.

As previously reported (White, 1987; Kullberg et al., 1990), omission of the δ subunit also changed the rectification of the macroscopic ACh-induced I-V relation in NaCl (Fig. 7 B). The I-V relation for $\alpha\beta\gamma$ in NaCl shown in Fig. 7 A was replotted in Fig. 7 B along with the curve for $\alpha\beta\gamma\delta$ shown in Fig. 4 B. The I-V relation for $\alpha\beta\gamma\delta$ from Fig. 4 B was normalized to the current for $\alpha\beta\gamma$ at -117 mV after matching the

TABLE II

Effects of Subunit Substitutions and Deletions

Receptor type	$V_r(\text{Tris}) - V_r(\text{Na})$	$P_{\text{Tris}}/P_{\text{Na}}$	n
	mV		
$\alpha\beta\gamma\delta$ (WT)	-27 ± 3*	0.36 ± 0.04*	59
$\alpha\beta\delta\epsilon$	-29 ± 4	0.33 ± 0.05	13
$\alpha\beta\delta\epsilon_5$	-30 ± 3	0.32 ± 0.04	4
$\alpha\beta\delta$	-29 ± 4	0.33 ± 0.04	6
$\alpha\beta\gamma$	-75 ± 7	0.06 ± 0.02	20
$\alpha\beta\gamma\delta_X$	-79 ± 11	0.05 ± 0.03	9
$(\alpha\beta\gamma\delta)_T$	-39 ± 5	0.22 ± 0.05	4

*Mean $\pm$ SD.

reversal potentials. Fig. 7 B shows that the I-V relation for the δ_0 receptor rectified more strongly than did the relation for the WT.

The $\alpha\beta\delta$, $\alpha\beta\delta\epsilon$, and $\alpha\beta\delta\epsilon_5$ receptors had approximately the same relative permeabilities to Tris$^+$ as $\alpha\beta\gamma\delta$ (Table II). Fig. 7 C shows I_{ACh} in NaCl and in Tris·HCl from an oocyte injected with $\alpha\beta\delta$ after a 7-d incubation. I_{ACh} reversed at -4 mV in NaCl and at -29 mV in Tris·HCl, giving a $P_{\text{Tris}}/P_{\text{Na}}$ of 0.38.

Normalized, ACh-induced I-V relations for $\alpha\beta\delta$ (γ_0) and $\alpha\beta\gamma\delta$ in NaCl are shown in Fig. 7 D. As reported by Charnet et al. (1992), omitting γ had no noticeable effect on the rectification of I_{ACh} in NaCl. The I-V relation for γ_0 in Fig. 7 D essentially superimposed on the WT curve.

Point Mutation Data Predict Subunit Alteration Data

The effects of the point mutations were consistent with effects of the subunit omissions and substitutions given (*a*) the hypothesis that positions $-1'$ and $2'$ form the main ion selectivity filter of the nAChR, and (*b*) the present view that γ substitutes for δ in the δ_0 channels and vice-versa (Kullberg et al., 1990; Charnet et al., 1992).

Under this assumption, γ_0 channels would correspond to the double mutant $\alpha\beta\gamma_{Q-1'E,T2'S}\delta$ (at positions $-1'$ and $2'$), and δ_0 channels would correspond to the double mutant $\alpha\beta\gamma\delta_{E-1'Q,S2'T}$ (see Fig. 1). We did not construct these double mutants but we did measure the relative $Tris^+$ permeabilities of the appropriate single
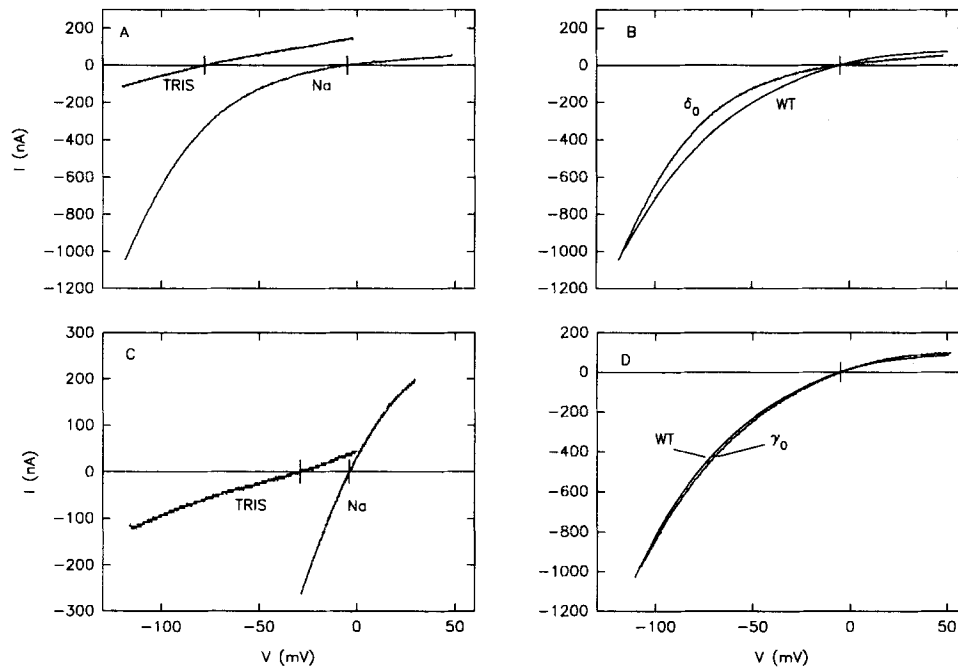

FIGURE 7. ACh-induced I-V relations for the WT ($\alpha\beta\gamma\delta$), δ_0 ($\alpha\beta\gamma$), and γ_0 ($\alpha\beta\delta$) receptors. Reversal potentials are indicated by vertical lines. Horizontal line indicates $I = 0$ nA. Scaling of voltage axis is identical in all panels. Note change of current scale in C. (A) ACh-induced I-V relations for $\alpha\beta\gamma$ in NaCl and in Tris·HCl. The I-V relation in NaCl was generated by ramping the voltage from -120 to $+50$ mV and applying 3 μM ACh. The relation in Tris·HCl was generated by ramping the voltage from -120 to 0 mV and applying 50 μM ACh. (B) Normalized ACh-induced I-V relations for $\alpha\beta\gamma$ and $\alpha\beta\gamma\delta$ in NaCl. The original I-V relation for $\alpha\beta\gamma\delta$ in Fig. 4 B was shifted $+1$ mV along the voltage axis and the current was divided by a factor of 5.6 to match the current for $\alpha\beta\gamma$ at -117 mV. Curve for $\alpha\beta\gamma$ in NaCl was the same as in A. (C) ACh-induced I-V relations for $\alpha\beta\delta$ in NaCl and Tris·HCl. The curve in NaCl was generated by ramping the voltage from -30 to $+30$ mV and applying 3 μM ACh. The curve in Tris·HCl was generated by ramping from -120 to 0 mV and applying 5 μM ACh. (D) ACh-induced I-V relations for $\alpha\beta\delta$ and $\alpha\beta\gamma\delta$ in NaCl. The I-V relation for $\alpha\beta\gamma$ was generated by applying 3 μM ACh and ramping from -120 to $+50$ mV. The curve for $\alpha\beta\gamma\delta$ (same as in Figs. 4 D and 7 B) was normalized to I_{ACh} for $\alpha\beta\delta$ at -108 mV, after shifting the original $\alpha\beta\gamma\delta$ I-V relation $+1$ mV along the voltage axis to equate the reversal potentials.

mutants. Neither $\alpha\beta\gamma_{Q-1'E}\delta$ nor $\alpha\beta\gamma_{T2'S}\delta$ had any significant effect on the relative permeability of the receptor to $Tris^+$, which was consistent with the results from the γ_0 injections. Both $\alpha\beta\gamma\delta_{E-1'Q}$ and $\alpha\beta\gamma\delta_{S2'T}$ significantly lowered mean P_{Tris}/P_{Na} as would be expected from the results for the δ_0 and $\alpha\beta\gamma\delta_X$ hybrid receptors ($\alpha\beta\gamma\delta_X$ was

equivalent to $\alpha\beta\gamma\delta_{S2'T}$ at positions $-1'$ and $2'$; see Fig. 1). If we make the additional assumptions that (a) positions $-1'$ and $2'$ are part of a single rate-limiting barrier for Tris$^+$ permeation, (b) mutations at positions $-1'$ and $2'$ have an additive effect on the height of the relative energy barrier to Tris$^+$, and (c) $[V_r(\text{Tris}) - V_r(\text{Na})]$ multiplied by the Faraday constant (F) gives the difference between the height of the major energy barriers for Tris$^+$ and Na$^+$ permeation through the nAChR (ΔG), then the change in ΔG produced by omitting δ should be equal to the sum of changes produced by the two mutants, $\alpha\beta\gamma\delta_{E-1'Q}$ and $\alpha\beta\gamma\delta_{S2'T}$:

$$\Delta G_{\alpha\beta\gamma} - \Delta G_{\alpha\beta\gamma\delta} = (\Delta G_{\alpha\beta\gamma\delta(E-1'Q)} - \Delta G_{\alpha\beta\gamma\delta}) + (\Delta G_{\alpha\beta\gamma\delta(S2'T)} - \Delta G_{\alpha\beta\gamma\delta})$$

where the subscripts of ΔG indicate the receptor type. Factoring out F and simplifying, we have:

$$\Delta V_{\alpha\beta\gamma} = \Delta V_{\alpha\beta\gamma\delta(E-1'Q)} + \Delta V_{\alpha\beta\gamma\delta(S2'T)} - \Delta V_{\alpha\beta\gamma\delta}$$

where $\Delta V = [V_r(\text{Tris}) - V_r(\text{Na})]$. Mean $\Delta V_{\alpha\beta\gamma}$ was -75 ± 7 mV (Table II) and mean $(\Delta V_{\alpha\beta\gamma\delta(E-1'Q)} + \Delta V_{\alpha\beta\gamma\delta(S2'T)} - \Delta V_{\alpha\beta\gamma\delta})$ was -89 ± 20 mV (using the means and SDs for the WT, $\alpha\beta\gamma\delta_{E-1'Q}$, and $\alpha\beta\gamma\delta_{S2'T}$ given above). Thus, mean $[V_r(\text{Tris}) - V_r(\text{Na})]$ for the δ_0 receptor was consistent with values predicted from the mean $[V_r(\text{Tris}) - V_r(\text{Na})]$ for $\alpha\beta\gamma\delta_{E-1'Q}$, $\alpha\beta\gamma\delta_{S2'T}$, and $\alpha\beta\gamma\delta$. The data are, however, insufficiently precise to rule out the possibility that additional differences between δ_0 and those receptors possessing a full complement of normal or mutated subunits may also influence $P_{\text{Tris}}/P_{\text{Na}}$.

Substitution of ϵ for γ resulted in no change in the amino acids at position $-1'$ or $2'$ (see Fig. 1), and did not change the relative permeability of the channel to Tris$^+$.

Mole-Fraction Dependence of V_r Conforms to the GHK Equation

To see how well the behavior of the WT and δ_0 channels conformed to the predictions of the Goldman-Hodgkin-Katz (GHK) voltage equation, we measured the shift in the biionic reversal potential of I_{ACh} in mixed Na$^+$/Tris$^+$ solutions $[V_r(\text{Tris} + \text{Na}) - V_r(\text{Na})]$ as a function of the mole fraction of Tris$^+$ (Fig. 8 A). $[V_r(\text{Tris} + \text{Na}) - V_r(\text{Na})]$ was measured for a group of oocytes injected with $\alpha\beta\gamma\delta$ or $\alpha\beta\gamma$ in solutions made by replacing 0, 25, 50, 75, or 100% of the external Na$^+$ with Tris$^+$. We added -0.5 mV (59 mV·log [98/100]) to the values of $[V_r(\text{Tris} + \text{Na}) - V_r(\text{Na})]$ for 100% Na$^+$ replacement to compensate for the difference between the concentration of Na$^+$ (100 mM) and Tris$^+$ (98 mM) in the external solutions. The lines in Fig. 8 A represent least-squares fits of the raw data to the following equation, derived from the GHK voltage equation:

$$V_r(\text{Tris}) - V_r(\text{Na}) = 59 \log \left[1 - \left(1 - \frac{P_{\text{Tris}}}{P_{\text{Na}}} \right) \left(\frac{[\text{Tris}^+]}{[\text{Tris}^+] + [\text{Na}^+]} \right) \right] \tag{1}$$

where $[\text{Tris}^+]$ and $[\text{Na}^+]$ were the external concentrations. $[\text{Tris}^+]/([\text{Tris}^+] + [\text{Na}^+]) = 0$ was not included in the fit. Eq. 1 fit both the δ_0 and WT data well, but the fit to δ_0 was slightly better than that to the WT. Estimated $P_{\text{Tris}}/P_{\text{Na}}$ was 0.07 ± 0.004 ($\pm$ SEE) for δ_0 ($n = 42$ oocytes), and 0.32 ± 0.01 for the WT ($n = 36$). These estimates were close to the ones made by completely replacing external Na$^+$ with Tris$^+$ (0.36 ± 0.4 for $\alpha\beta\gamma\delta$ and 0.06 ± 0.2 for $\alpha\beta\gamma$). However, there was a slight, but noticeable,

discrepancy between the observed values of $[V_r(\text{Tris} + \text{Na}) - V_r(\text{Na})]$ for the WT and those extrapolated from the data for complete replacement of external Na^+ by Tris^+ using Eq. 1 (Fig. 8 *B*). The solid and dashed lines in Fig. 8 *B* show $[V_r(\text{Tris} + \text{Na}) - V_r(\text{Na})]$ calculated from Eq. 1 using the value for $P_{\text{Tris}}/P_{\text{Na}}$ calculated from the mean $[V_r(\text{Tris} + \text{Na}) - V_r(\text{Na})] \pm 2$ SD $(-28.4 \pm 3.6$ mV, $n = 13)$ for complete Na^+ replacement. The extrapolated values slightly underestimate the observed
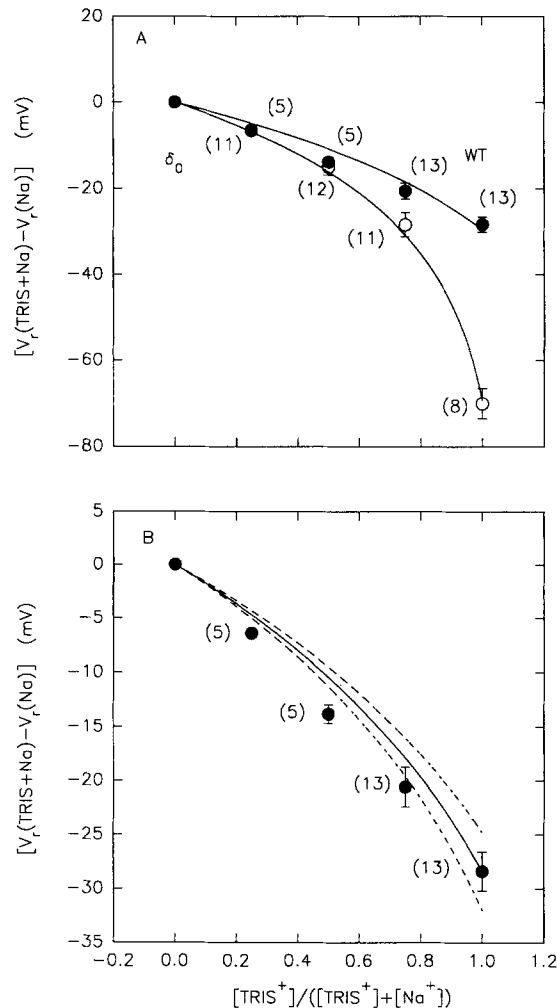

FIGURE 8. Shift in the reversal potential of I_{ACh}, $[V_r(\text{Tris} + \text{Na}) - V_r(\text{Na})]$, as a function of the mole-fraction of Tris^+, $[\text{Tris}^+]/([\text{Tris}^+] + [\text{Na}^+])$. Relevant sample sizes are given in parentheses. Error bars are ± 1 SD. (*A*) $[V_r(\text{Tris} + \text{Na}) - V_r(\text{Na})]$ versus $[\text{Tris}^+]/([\text{Tris}^+] + [\text{Na}^+])$ for the mouse WT (filled circles) and δ_0 (hollow circles). Total n was 13 for the WT and 12 for δ_0. Lines are least-squares fits of the raw data using Eq. 1 in the text. (*B*) Observed mean $[V_r(\text{Tris} + \text{Na}) - V_r(\text{Na})]$ for the WT versus the values predicted by complete replacement of Na^+ by Tris^+. Solid line represents $[V_r(\text{Tris} + \text{Na}) - V_r(\text{Na})]$ predicted from the GHK voltage equation (Eq. 1) and mean $P_{\text{Tris}}/P_{\text{Na}}$ estimated by replacing 100 mM Na^+ with 98 mM Tris^+. Dashed lines represent mean $P_{\text{Tris}}/P_{\text{Na}} \pm 2$ SD.

$[V_r(\text{Tris} + \text{Na}) - V_r(\text{Na})]$ at 25, 50, and 75% Tris^+, and $[V_r(\text{Tris} + \text{Na}) - V_r(\text{Na})]$ was actually closer to a linear function of $[\text{Tris}^+]/([\text{Tris}^+] + [\text{Na}^+])$ than to the logarithmic function predicted by Eq. 1. Thus, even though the mole-fraction data conformed approximately to the predictions of the GHK equation, there was a slight departure from GHK behavior for the WT receptor. Previous studies of ACh-induced, whole-cell (Fiekers and Henderson, 1982) and single-channel (Sanchez, Dani, Siemen, and

Hille, 1986) currents have also shown discrepancies between the observed currents in mixed $Na^+/Tris^+$ solutions and the predictions of the GHK current equation.

Effect of Reducing δ

One possible interpretation of some of the mutation data is that δ mutations simply reduced the probability of incorporating δ into the receptor and therefore increased the proportion of δ_0 channels in the population. Theoretically, such an increase could reduce the apparent relative permeability of the total nAChR population to $Tris^+$ even if the mutations themselves had no direct effect on P_{Tris}/P_{Na}. To test this hypothesis, we measured [V_r(Tris) − V_r(Na)] and P_{Tris}/P_{Na} for oocytes with one of the following ratios of α:β:γ:δ: (a) 2:1:1:1, (b) 2:1:1:0.2, or (c) 2:1:1:0.1.

Reducing δ by 1/5 or 1/10 reduced the amplitude of the ACh response but had no effect on the relative $Tris^+$ permeability. Mean [V_r(Tris) − V_r(Na)] was −29 ± 2 mV with the normal concentration of δ (n = 14), −28 ± 3 mV for 1/5 δ (n = 14), and −31 ± 5 mV for 1/10 δ (n = 13); and mean P_{Tris}/P_{Na} was 0.34 ± 0.03, 0.34 ± 0.04, and 0.31 ± 0.06. There were no significant differences between mean [V_r(Tris) − V_r(Na)] (P ≥ 0.08) or P_{Tris}/P_{Na} (P ≥ 0.15) among the three groups. Thus, reducing the concentration of δ by 90% did not lower the apparent relative permeability of αβγδ to $Tris^+$.

Single-Channel Recordings

To determine if the $αβγδ_{S2'F}$ mutant resulted in the formation of a new channel type or merely represented a composite of WT and $δ_0$ channels, we recorded single nAChR openings in patches containing WT or $αβγδ_{S2'F}$ channels. Fig. 9, A and B show examples of single-channel I-V relations for αβγδ (Fig. 9 A) and $αβγδ_{S2'F}$ (Fig. 9 B) created by ramping the command potential of the patch clamp between −150 and +150 mV. Single-channel currents for both αβγδ (Leonard et al., 1988) and $αβγδ_{S2'F}$ rectified inwardly. The slope conductance of the main conductance at negative holding potentials (solid lines in Fig. 9, A and B) was 40 pS for αβγδ and 33 pS for $αβγδ_{S2'F}$ for the patches in Fig. 9, A and B.

As is evident from Fig. 9 A, the WT receptor (αβγδ) had several conductance states, but further study indicated that none of these states matched the main state conductance of $αβγδ_{S2'F}$ at 13 or 23°C. At 13°C, αβγδ displayed three different conductance states in six patches with mean conductances of 43 ± 4 pS (n = 3 patches), 22 ± 1 pS (n = 3), and 13 pS (n = 1), while $αβγδ_{S2'F}$ had a 32 ± 1-pS main state conductance (n = 2) and an 11-pS substate (n = 1) in two patches. At 23°C, αβγδ had a main state conductance of 65 ± 2 pS (n = 7) and a substate conductance of 14 ± 1 pS (n = 2), while $αβγδ_{S2'F}$ had a main state conductance of 50 pS and a substate conductance of 28 pS (n = 1). Thus, the main state of $αβγδ_{S2'F}$ was distinct from all the identifiable conductance states of αβγδ.

The temperature dependence of the main state of αβγδ and the largest conductance state of $αβγδ_{S2'F}$ were nearly identical. Assuming that the 43-pS state at 13°C and the 65-pS state at 23°C represented the same state, the Q_{10} for the largest conductance state of αβγδ was 1.5. Similarly, assuming that the 32-pS state at 13°C and the 50-pS state at 23°C were the same channel, the Q_{10} of $αβγδ_{S2'F}$ was 1.6. Thus, single-channel recordings showed that the $αβγδ_{S2'F}$ mutation resulted in the appear-

ance of a distinct channel type with a smaller conductance than the main state of αβγδ but a similar temperature dependence.

There Were Many Unresponsive Mutants

Charnet et al. (1990) found that several mutants at position 2′ failed to express functional receptors. This pattern continued in our studies. However, by using higher
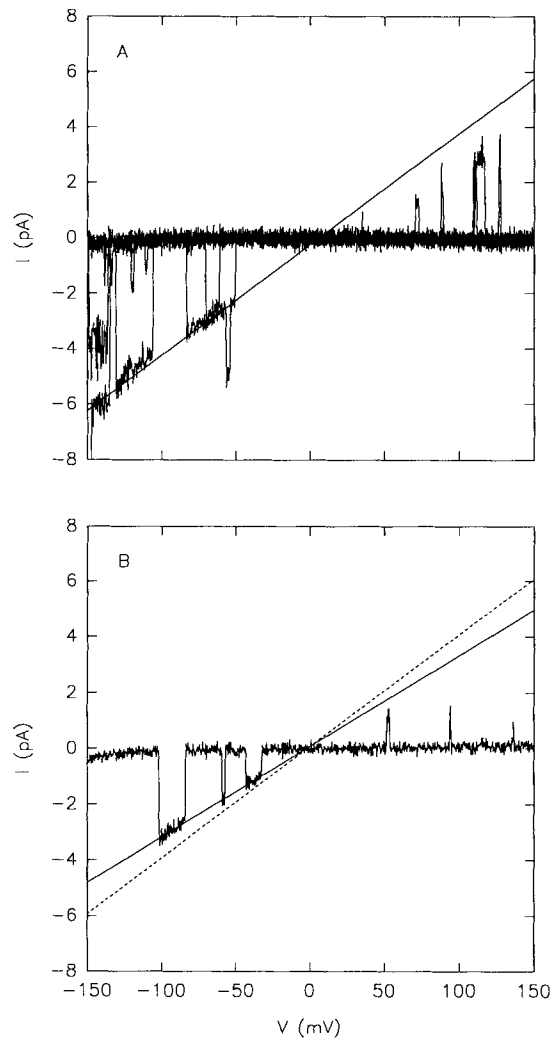

FIGURE 9. *I-V* relations for single ACh channel openings generated by ramping the patch voltage in a symmetrical KCl solution (see Methods) at 13°C. Background current was subtracted out by fitting a straight line to a region without channel activity (−25 to +35 mV). Sampling frequency was 3.3 kHz. (*A*) Single-channel *I-V* relation for αβγδ. The data from seven successive ramps are superimposed. Filter $f_c = 1$ kHz. Solid line shows the slope conductance of the main state currents at negative holding potentials. [ACh] = 1 μM. The extrapolated reversal potential (V_r) was +6 mV. (*B*) Single-channel *I-V* relation for αβγδ$_{S2'F}$. Data are from one ramp. The αβγδ$_{S2'F}$ channels quickly desensitized at the high ACh concentration (100 μM) required to see activity. Filter $f_c = 0.8$ kHz. Solid line gives the slope conductance of αβγδ$_{S2'F}$, and the dashed line gives the slope conductance of αβγδ, shifted to V_r for αβγδ$_{S2'F}$ (−3 mV).

ACh concentrations than previously, we obtained data from two mutants ($α_{T2'A}βγ_{T2'A}δ$, $α_{T2'A}βγδ_{S2'A}$) that previously gave undetectable responses. A third mutant ($α_{T2'A}βγ_{T2'A}δ_{S2'A}$) still failed to respond to higher agonist concentrations.

Mutations at positions −1′ or 2′ in α were more likely to abolish agonist responses completely than were similar mutations in γ or δ. In addition, mutations at position

$2'$ in δ were more likely to abolish agonist response in Tris·HCl than were similar mutations in γ. 12 of 39 $\alpha\beta\gamma\delta$ mutants did not respond to 0.1–2 mM ACh in NaCl: $\alpha_{E-1'Q}\beta\gamma\delta$, $\alpha_{T2'L}\beta\gamma\delta$, $\alpha_{T2'F}\beta\gamma\delta$, $\alpha_{T2'Y}\beta\gamma\delta$, $\alpha_{T2'G}\beta\gamma\delta$, $\alpha_{T2'S}\beta\gamma\delta$, $\alpha\beta\gamma\delta_{S2'C}$, $\alpha\beta\gamma\delta_{S2'L}$, $\alpha_{T2'A}\beta_{G2'S}\gamma_{T2'A}$ $\delta_{S2'A}$, $\alpha\beta\gamma_{Q-1'E}\delta_{E-1'Q}$, $\alpha_{T2'A}\beta\gamma_{T2'A}\delta_{S2'A}$, and $\alpha_{F14'S}\beta_{F14'Y}\gamma_{F14'S}\delta_{F14'S}$. Mutants that did not respond in NaCl were usually not tested further with Tris·HCl. In addition to the above mutants, two δ mutants responded to ACh in NaCl but failed to respond in Tris·HCl: $\alpha\beta\gamma\delta_{S2'Y}$ and $\alpha\beta\gamma\delta_{S2'G}$. All in all, six of the seven point mutations we made at positions $-1'$ and $2'$ in α completely abolished agonist responses, and four of eight similar mutations in δ abolished agonist responses in Tris·HCl. In contrast, all six receptors with a single mutation in γ at position $-1'$ or $2'$ ($\alpha\beta\gamma_{Q-1'E}\delta$, $\alpha\beta\gamma_{T2'A}\delta$, $\alpha\beta\gamma_{T2'S}\delta$, $\alpha\beta\gamma_{T2'L}\delta$, $\alpha\beta\gamma_{T2'F}\delta$, and $\alpha\beta\gamma_{T2'Y}\delta$), and the single receptor with a comparable mutation in β ($\alpha\beta_{G2'S}\gamma\delta$), gave robust ACh responses in both NaCl and Tris·HCl. The subunit stoichiometry of the channel (presumably $\alpha:\beta:\gamma:\delta = 2:1:1:1$) may explain the effects of mutations in α on receptor expression. The finding that fewer δ than γ mutants responded in Tris·HCl was consistent with the effects of position $2'$ mutations on relative Tris$^+$ permeability.

We did not pursue further tests of mutant expression using [^{125}I]α-bungarotoxin (Yoshii et al., 1987) because we found that this assay was far less sensitive than the electrophysiological assay. Mutants such as $\alpha\beta\gamma\delta_{S2'F}$, which gave easily detectable ACh responses, displayed barely detectable [^{125}I]α-bungarotoxin binding. Thus, it is possible that some of the mutant mRNA combinations led to receptors that are fully assembled, can bind ACh, and can undergo the conformational changes that normally open the channel, but cannot pass Na$^+$ or Tris$^+$.

DISCUSSION

We measured the relative permeability of WT and mutated nAChR's to Tris$^+$ electrophysiologically. The results support the hypothesis that M2 is the pore-forming region of the nAChR and suggest that positions $-1'$ and $2'$ in M2 probably form the main ion selectivity filter of the channel for large monovalent cations. We also found that increasing the hydrophobicity of the residues at position $2'$ without increasing the volume is sufficient to lower dramatically the relative Tris$^+$ permeability of the channel. In fact, side-chain hydrophobicity at position $2'$ is a better overall predictor of the relative Tris$^+$ permeability than is side-chain volume. A comparison of mutations at position $2'$ in δ and γ suggests that δ plays a more important role in ion selectivity than γ.

Our results also show that subunit deletions and substitutions can change the ion selectivity of the mouse nAChR. The δ_0 receptor and the mouse-*Xenopus* hybrid $\alpha\beta\gamma\delta_X$ are almost impermeable to Tris$^+$, while the γ_0, $\alpha\beta\delta\epsilon$, and $\alpha\beta\delta\epsilon_5$ receptors have the same relative permeability to Tris$^+$ as $\alpha\beta\gamma\delta$.

Finally, we found that the mole-fraction dependence of the biionic reversal potential of I_{ACh} in mixed Na$^+$/Tris$^+$ solutions was described reasonably well by the GHK voltage equation, with the possibility of a slight departure by the mouse WT nAChR.

Ion Selectivity Filter Is at Positions $-1'$ and $2'$

The Li$^+$/NH$_4^+$ permeability ratio is constant for concentrations between 10 and 150 mM, and streaming potentials are rather small for large organic cations (Dani, 1989).

These facts suggest that nAChR's in BC3H-1 cells have a single main site for ion–channel interaction, 3–6 Å long, that is either a binding site or a barrier for ions permeating the channel (Dani, 1989). Our experiments identify positions $-1'$ and $2'$ as the major site of Tris$^+$ selectivity. An idealized α-helix has 3.6 residues per turn and a pitch of 5.4 Å (Pauling, Corey, and Branson, 1951), and in some models the predicted α-helical conformation of M2 extends to position $-1'$ (Furois-Corbin and Pullman, 1988; Hilgenfeld and Hucho, 1988). The molecular dimensions of Tris$^+$ are 6.0 × 6.9 × 7.7 Å (Huang et al., 1978), which means that a Tris$^+$ molecule might simultaneously contact the side chains at both positions $-1'$ and $2'$, depending on their exact conformations. Thus, positions $-1'$ and $2'$ could be part of a single site that interacts with large organic cations. Therefore, both the streaming potential measurements and our mutation data are consistent with the hypothesis that the main selectivity filter for large monovalent cations could be localized to one full turn of the M2 α-helix.

The monotonic decline in V_r in the mole-fraction experiments is consistent with the hypothesis that $\alpha\beta\gamma\delta$ and δ_0 can hold only one ion at a time (Eisenman and Dani, 1987). A one-ion channel may nonetheless contain more than one energy well (ion-binding site) and energy barrier for a permeating ion (Läuger, 1973). The fair agreement between the shift in V_r produced by varying the mole-fraction of Tris$^+$ and the GHK voltage equation (Eq. 1, Fig. 8, *A* and *B*) suggests that δ_0 and $\alpha\beta\gamma\delta$ contain either (*a*) a single, rate-limiting barrier for permeation or (*b*) multiple energy barriers whose heights for Na$^+$ and Tris$^+$ permeation differ by a constant amount for the two ions (constant energy offset condition [Läuger, 1973; Hille, 1975; Levitt, 1986]).

We should, however, avoid an oversimplified view of Na$^+$ and Tris$^+$ permeation. First, Fig. 8 *B* does show small deviations between Tris$^+$/Na$^+$ permeability ratios for $\alpha\beta\gamma\delta$ and the predictions of Eq. 1. These deviations could be caused by (*a*) a slight difference in the location of the rate-limiting barrier for Na$^+$ and Tris$^+$ permeation in the electric field of the channel, or (*b*) a small deviation from the constant energy offset condition (Krasne, 1980). Second, the region between positions $-1'$ and $2'$ is not the sole determinant of ion selectivity. The $\alpha\beta_{G2'S}\gamma\delta$ mutant receptor has the same amino acids at position $-1'$ and $2'$ as $(\alpha\beta\gamma\delta)_T$, but the same relative permeability to Tris$^+$ as $\alpha\beta\gamma\delta$. If we assume that differences in the overall conformation of $(\alpha\beta\gamma\delta)_T$ are not responsible for the difference in the selectivity of $\alpha\beta\gamma\delta$ and $(\alpha\beta\gamma\delta)_T$, then there must be additional sites in the channel that influence its selectivity for large monovalent cations.

Hydrophobicity Influences Ion Selectivity

Previous work on nAChR's at the frog neuromuscular junction (Dwyer et al., 1980) has shown that the relative permeability of the nAChR to organic cations decreases monotonically with the size of the cation, as though ion selectivity is primarily determined by an increase in the hydrodynamic friction between a permeating ion and the channel wall. Our results showing a weak correlation between the change in side-chain volume at position $2'$ and the Tris$^+$/Na$^+$ permeability ratio emphasize hydrophobicity instead. Replacing the amino acids at position $2'$ with much larger residues, such as phenylalanine and tyrosine, significantly reduced the relative permeability of the channel to Tris$^+$; but these mutations also changed the hydropho-

bicity of residues at position 2', and our results show that a significant reduction in relative Tris$^+$ permeability can be obtained without increasing the volume of the residues at position 2'. In fact, two of the five mutants listed in Table I with the lowest relative permeabilities to Tris$^+$ ($\alpha_{T2'A}\beta\gamma\delta_{S2'A}$ and $\alpha_{T2'A}\beta_{G2'S}\gamma\delta_{S2'A}$) were mutants that did not involve increases in the total side-chain volume at position 2'. Mean P_{Tris}/P_{Na} for $\alpha_{T2'A}\beta\gamma\delta_{S2'A}$ (0.13 ± 0.04) was 64% less than for the WT (0.36 ± 0.2), and mean P_{Tris}/P_{Na} for $\alpha_{T2'A}\beta_{G2'S}\gamma\delta_{S2'A}$ (0.15 ± 0.02) was 58% less. However, an increase in the hydrophobicity of the amino acids at position 2' could allow residues with the same or a smaller volume to pack more closely together, thus constricting the pore. High-resolution structural data are evidently required to decide whether the reduction in relative Tris$^+$ permeability produced by raising the hydrophobicity of the position 2' residues is due to a constriction of the pore or to some other mechanism.

Nevertheless, the strong correlation between relative hydrophobicity of the residues at position 2' and the Tris$^+$/Na$^+$ permeability ratios of mutant receptors with $\Sigma V \leq \Sigma V_{WT}$ suggests that one should consider the role of hydrogen bonds between a permeant ion and the position 2' residues and/or the electrostatic repulsion between a large cation and the walls of the channel as factors in determining selectivity. Replacing the serines and threonines with nonpolar amino acids at position 2' reduces the number of residues available for hydrogen bonding to Tris$^+$ at this position. Assuming that large cations such as Tris$^+$ must be dehydrated more completely than small ions such as Na$^+$, reducing the number of position 2' residues available for hydrogen bonding would increase the added energy required for Tris$^+$ to permeate the channel. The result could be a lower Tris$^+$/Na$^+$ permeability ratio. The energy represented by the difference between $[V_r(Tris) - V_r(Na)]$ for $\alpha\beta\gamma\delta$ and $\alpha_{T2'A}\beta\gamma\delta_{S2'A}$ is 0.64 kcal/mol. This energy is at the low end of the range of estimated energies (0.5–1.8 kcal/mol) for hydrogen bonds between uncharged donors and acceptors in protein–ligand complexes and nucleic acids (Alber, 1989). Alternatively, increased electrostatic repulsion between the channel walls and Tris$^+$ could account for the lower relative Tris$^+$ permeability. The nAChR pore is supposed to be large enough (minimum of 6.5 Å across at its narrowest constriction) to accommodate a small cation such as Na$^+$ without complete dehydration. Thus, it is possible that Na$^+$ is partially shielded from changes in the dielectric constant of the channel wall by water molecules, while a large cation such as Tris$^+$ is not shielded.

γ and δ Play Nonequivalent Roles

One possible explanation for the apparent difference between the effects of mutations at position 2' in γ and δ is the difference between the residues at position $-1'$ in these two subunits. The γ subunit has an uncharged glutamine (Q) at position $-1'$, while the δ subunit has a negatively charged glutamate (E) at this position (see Fig. 1). If positions $-1'$ and 2' form part of a single binding site for Tris$^+$, then mutations at position 2' in γ might be less disruptive than mutations at the same position in δ because Tris$^+$ binding is normally weaker to γ as a result of the uncharged amino acid at position $-1'$.

An alternative explanation for the difference between γ and δ is that the subunits are asymmetrically arranged around the pore, possibly because of the additional residue that appears uniquely in the γ sequence at position $-2'$ (not shown in Fig. 1).

Thus, position 2' in γ might be less accessible to Tris$^+$ than the corresponding position in δ because of the way γ is tilted relative to the pore axis, but position $-1'$ in γ might be more accessible. In support of a different configuration for the γ subunit, previous work (Imoto et al., 1988) has shown that mutating the glutamine at position $-1'$ in the *Torpedo* γ subunit to lysine reduced the single-channel conductance more than was expected on the basis of the net charge change at that position.

Conductance States of $\alpha\beta\gamma\delta$ and $\alpha\beta\gamma\delta_{S2'F}$

The single-channel data show that the WT ($\alpha\beta\gamma\delta$) and $\alpha\beta\gamma\delta_{S2'F}$ mutations clearly display different main-state conductances; other mutations at position 2' have also produced conductance changes (Villarroel et al., 1991).

Previous data (Kullberg et al., 1990) suggest that the multiple conductance states observed for WT nAChR's, cloned from BC3H-1 cells and expressed in oocytes, represent distinct subunit compositions. More measurements will be necessary to correlate the substrates in our mutated channels with particular subunit compositions.

Subunit Deletions and Point Mutations Give Complementary Data

Our results show that deletions or substitutions of the δ, but not γ, subunit dramatically reduce the relative permeability of the channel to Tris$^+$. This result raises the question of whether or not some of the point mutation data could arise artifactually from the formation of nAChR's with subunit deletions. The formation of γ_0 channels clearly cannot account for the effects of point mutations at position 2', because the γ_0 receptor has the same relative permeability to Tris$^+$ as the WT channel. The absence of an effect of reducing the relative concentration of δ on the relative permeability of $\alpha\beta\gamma\delta$ to Tris$^+$ and the difference between the main-state conductance of $\alpha\beta\gamma\delta$ and $\alpha\beta\gamma\delta_{S2'F}$ argues that δ_0 channels do not account for the effects of all the mutations in δ. Furthermore, the effects of the point mutations are consistent with effects of the subunit deletions if we assume that γ substitutes for δ in δ_0 channels, and vice-versa (Kullberg et al., 1990). Finally, the incubation times of the δ mutants were generally shorter than that required to obtain ACh responses from δ_0. These data do not formally exclude the possibility, but render it quite unlikely, that the formation of δ_0 channels provides a trivial explanation for our graded effects of point mutations in the δ subunit.

A Number of Experiments Suggest That M2 Lines the Pore

Fig. 10, *A* and *B*, gives a structure–function map of M2 based on the results of this and previous studies. Previous work shows that mutations at positions $-1'$, 2', 6', and 20' affect single-channel conductance (Imoto et al., 1988; Leonard et al., 1988; Charnet et al., 1990; Villarroel et al., 1991); mutations at position $-1'$, 2', and 20' affect monovalent metal cation selectivity (Konno et al., 1991; Villarroel et al., 1991); mutations at position 20' affect block by Mg^{2+} (Imoto et al., 1988); and mutations at positions 6' and 10' affect block by QX-222 (Leonard et al., 1988; Charnet et al., 1990). Our experiments show that mutations at positions $-1'$ and 2' alter the selectivity of the channel for Tris$^+$ (present results) and for other large organic cations (Cohen, B. N., C. Labarca, L. Czyzyk, N. Davidson, and H. A. Lester,

A

	-1	0	1	2	3	4	5	6	7	8	9	10	11	12	13	14	15	16	17	18	19	20	21
α	E	K	M	T	L	S	I	S	V	L	L	S	L	T	V	F	L	L	V	I	V	E	L
β	E	K	M	G	L	S	I	F	A	L	L	T	L	T	V	F	L	L	L	L	A	D	K
γ	Q	K	C	T	V	A	T	N	V	L	L	A	Q	T	V	F	L	F	L	V	A	K	K
δ	E	K	T	S	V	A	I	S	V	L	L	A	Q	S	V	F	L	L	L	I	S	K	R

B

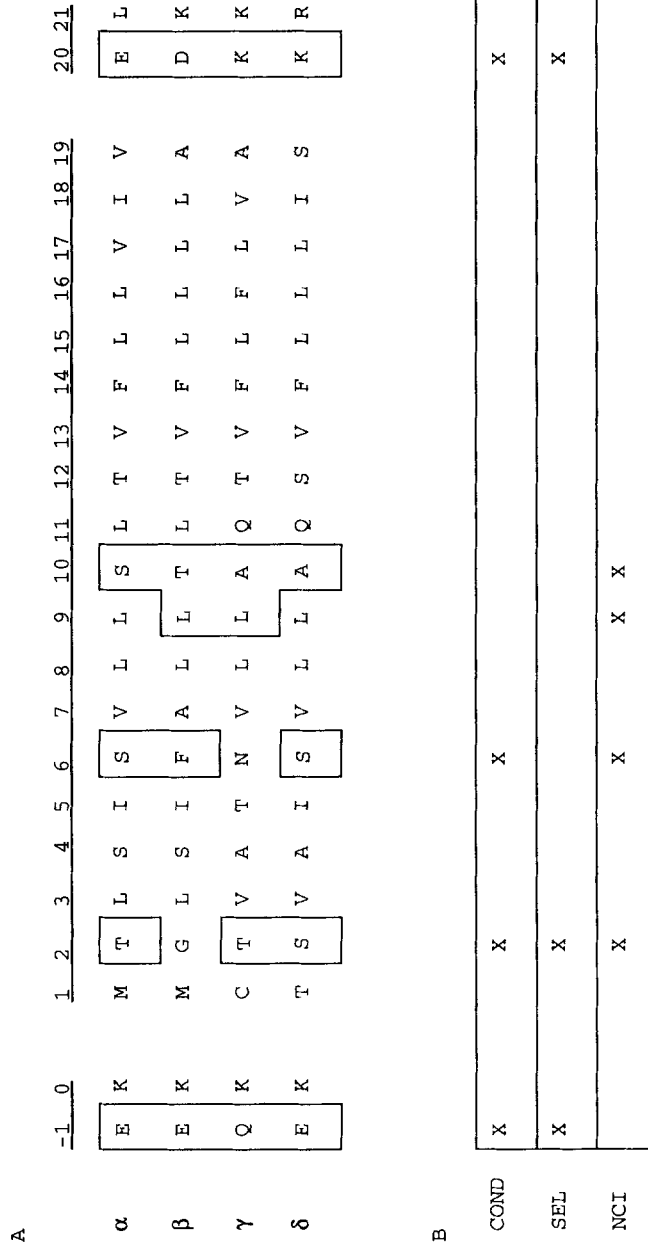|	1	6		9 10		20
COND	X	X				X
SEL	X	X				X
NCI	X	X		X X		

FIGURE 10. Structure–function map of mouse M2 and adjoining residues. (A) M2 sequence. Outlined residues in M2 affect single-channel conductance (COND), ion selectivity (SEL), or noncompetitive inhibitor binding (NCI). (B) Functions (COND, SEL, or NCI) attributed to M2 positions. They are indicated by an X in the appropriate column and row. See text for references.

unpublished data). These functions are all normally associated with the conducting pore of the nAChR channel. Other noncompetitive inhibitors (NCIs), [^{3}H]chlorpromazine (Giraudat et al., 1986; Giraudat, Dennis, Heidmann, Haumont, Lederer, and Changeux, 1987; Giraudat, Galzi, Revah, Changeux, Haumont and Lederer, 1989; Revah et al., 1990) and [^{3}H]triphenylmethylphosphonium (Hucho, Oberthür, and Lottspeich, 1986; Oberthür et al., 1986), photolabel positions 2', 6', and 9' in the *Torpedo* M2. These compounds are also thought to act as channel blockers.

The residues in Fig. 10 A that affect channel functions between positions −1' and 10' are spaced three to four amino acids apart as would be expected from an α-helical secondary structure. At present, no function has been attributed to position 14' despite previous modeling of the pore which suggests that the phenylalanines at this position could act as a cation binding site (Eisenman et al., 1990). An obvious cautionary note is that this spacing also reflects the particular emphasis of the mutants that have been made and tested, although some attention has been paid to other positions (Charnet et al., 1990; Villarroel et al., 1991; this paper).

Our view (reviewed in Lester, 1992) is that the five M2 α-helices surround the conducting pore like sheaves of wheat, slightly askew so that there is a point of closest approach. At the extracellular vestibule, fixed charges affect ion flux. The open channel blocker, QX-222, penetrates partially into the tapering channel, so that its nonpolar aromatic moiety interacts most strongly with position 10' and its polar moiety interacts most strongly with position 6'. Permeant ions also interact with the residues at position 6'. The taper of the channel, or the absence of a hydrophobic binding site for the aromatic moiety at position 6', prevents QX-222 from reaching the next helical turn at position 2'. Here and at the next turn (position −1') the channel is narrowest; and the M2 residues interact most strongly with permeant ions. The channel widens after position −1' but conductance is still affected by the ring of charged amino acids at position −4'. We eagerly await the humiliation that will result from high resolution structural data.

REFERENCES

Adams, D. J., T. M. Dwyer, and B. Hille. 1980. The permeability of endplate channels to monovalent and divalent metal cations. *Journal of General Physiology.* 75:493–510.

Alber, T. 1989. Stabilization energies of protein conformation. *In* Prediction of Protein Structure and the Principles of Protein Conformation. Plenum Publishing Corp., New York. 161–192.

Baldwin, T. J., C. M. Yoshihara, K. Blackmer, C. R. Kintner, and S. J. Burden. 1988. Regulation of acetylcholine receptor transcript expression during development in *Xenopus laevis. Journal of Cell Biology.* 106:469–478.

Barish, M. E. 1983. A transient calcium-dependent chloride current in the immature *Xenopus* oocyte. *Journal of Physiology.* 342:309–325.

Charnet, P., C. Labarca, R. J. Leonard, N. J. Vogelaar, L. Czyzyk, A. Gouin, N. Davidson, and H. A.

Lester. 1990. An open-channel blocker interacts with adjacent turns of α-helices in the nicotinic acetylcholine receptor. *Neuron*. 4:87–95.

Charnet, P., C. Labaraca, and H. A. Lester. 1992. Structure of the γ-less nicotinic acetylcholine receptor: learning from omission. *Molecular Pharmacology*. In press.

Claudio, T., M. Ballivet, J. Patrick, and S. Heinemann. 1983. Nucleotide and deduced amino acid sequences of *Torpedo californica* acetylcholine receptor γ subunit. *Proceedings of the National Academy of Sciences, USA*. 80:1111–1115.

Cohen, B. N., C. Labarca, N. Davidson, and H. Lester. 1991. Ion selectivity of mutated and wild-type nicotinic ACh channels. *Biophysical Journal*. 59:33a. (Abstr.)

Creighton, T. E. 1984. Proteins. W. H. Freeman and Company, New York. 7.

Dani, J. A. 1989. Open channel structure and ion binding sites of the nicotinic acetylcholine receptor. *Journal of Neuroscience*. 9:884–892.

Dascal, N. 1987. Use of the *Xenopus* oocyte system to study ion channels. *CRC Critical Reviews in Biochemistry*. 22:317–387.

Dwyer, T. M., D. J. Adams, and B. Hille. 1980. The permeability of the endplate channel to organic cations in frog muscle. *Journal of General Physiology*. 75:469–492.

Eisenman, G., and J. A. Dani. 1987. An introduction to molecular architecture and permeability of ion channels. *Annual Review of Biophysics and Biophysical Chemistry*. 16:205–226.

Eisenman, G., A. Villarroel, M. Montal, and O. Alvarez. 1990. Energy profiles for ion permeation in pentameric protein channels: from viruses to receptor channels. *Progress in Cell Research*. 1:195–211.

Fiekers, J. F., and E. G. Henderson. 1982. Voltage clamp analysis of the effect of cationic substitution on the conductance of end-plate channels. *Pflügers Archiv*. 394:38–47.

Furois-Corbin, S., and A. Pullman. 1988. Theoretical study of potential ion-channels formed by bundles of α-helices. Partial modelling of the acetylcholine receptor channel. *In* Transport through Membranes: Carriers, Channels, and Pumps. A. Pullman, J. Jortner, and B. Pullman, editors. Kluwer Academic Publishers, Norwell, MA. 337–357.

Gardner, P. 1990. Nucleotide sequence of the ε-subunit of the mouse muscle nicotinic receptor. *Nucleic Acids Research*. 18:6714.

Giraudat, J., M. Dennis, T. Heidmann, J.-Y. Chang, and J.-P. Changeux. 1986. Structure of the high-affinity binding site for noncompetitive blockers of the acetylcholine receptor: serine-262 of the δ subunit is labeled by [^{3}H]chlorpromazine. *Proceedings of the National Academy of Sciences, USA*. 83:2719–2723.

Giraudat, J., M. Dennis, T. Heidmann, P. Haumont, F. Lederer, and J. Changeux. 1987. Structure of the High-affinity binding site for noncompetitive blockers of the acetylcholine receptor: [^{3}H]Chlorpromazine labels homologous residues in the β and δ chains. *Biochemistry*. 26:2410–2418.

Giraudat, J., J.-L. Galzi, F. Revah, J.-P. Changeux, P.-Y. Haumont, and F. Lederer. 1989. The noncompetitive blocker [^{3}H]chlorpromazine labels segment M2 but not segment M1 of the nicotinic acetylcholine receptor α-subunit. *FEBS Letters*. 253:190–198.

Good, N. E., G. D. Winget, W. Winter, T. Connolly, S. Izawa, and R. M. M. Singh. 1966. Hydrogen ion buffers for biological research. *Biochemistry*. 5:467–477.

Guy, H. R. 1985. Amino acid side-chain partition energies and distribution of residues in soluble proteins. *Biophysical Journal*. 47:61–70.

Hilgenfeld, R., and F. Hucho. 1988. Properties and problems of the helix-M2 model of the acetylcholine receptor-ion channel. *In* Transport through Membranes: Carriers, Channels and Pumps. A. Pullman, J. Jortner, and B. Pullman, editors. Kluwer Academic Publishers, Norwell, MA. 360–366.

Hille, B. 1975. Ionic selectivity of Na and K channels of nerve membranes. *In* Membranes: A Series of

Advances. Vol. 3. Lipid Bilayers and Biological Membranes: Dynamic Properties, G. Eisenman, editor. Marcel Dekker, Inc., New York. 255–323.

Huang, L. M., W. A. Catterall, and G. Ehrenstein. 1978. Selectivity of cations and nonelectrolytes for acetylcholine-activated channels in cultured muscle cells. *Journal of General Physiology.* 71:397–410.

Hucho, F., W. Oberthür, and F. Lottspeich. 1986. The ion channel of the nicotinic acetylcholine channel is formed by the homologous helices M II of the receptor subunits. *FEBS Letters.* 205:137–142.

Imoto, K., C. Busch, B. Sakmann, M. Mishina, T. Konno, J. Nakai, H. Bujo, Y. Mori, K. Fukuda, and S. Numa. 1988. Rings of negatively charged amino acids determine the acetylcholine receptor channel conductance. *Nature.* 335:645–648.

Isenberg, K. E., J. Mudd, V. Shah, and J. P. Merlie. 1986. Nucleotide sequence of the mouse muscle nicotinic acetylcholine receptor alpha subunit. *Nucleic Acids Research.* 14:5111.

Konno, T., C. Busch, E. von Kitzing, K. Imoto, F. Wang, J. Nakai, M. Mishina, S. Numa, and B. Sakmann. 1991. Rings of anionic amino acids as structural determinants of ion selectivity in the acetylcholine receptor channel. *Proceedings of the Royal Society of London, Series B.* 244:69–74.

Krasne, S. 1980. Ion selectivity in membrane permeation. *In* Membrane Physiology. T. E. Andreoli, J. F. Hoffman, and D. D. Fanestil, editors. Plenum Publishing Corp., New York. 217–241.

Kullberg, R., J. L. Owens, P. Camacho, G. Mandel, and P. Brehm. 1990. Multiple conductance classes of mouse nicotinic acetylcholine receptors expressed in *Xenopus* oocytes. *Proceedings of the National Academy of Sciences, USA.* 87:2067–2071.

LaPolla, R. J., K. S. Mixter-Mayne, and N. Davidson. 1985. Isolation and characterization of cDNA clone for the complete coding region of the δ subunit of the mouse acetylcholine receptor. *Proceedings of the National Academy of Sciences, USA.* 81:7970–7984.

Läuger, P. 1973. Ion transport through pores: a rate-theory analysis. *Biochimica et Biophysica Acta.* 311:423–441.

Leonard, R. J., C. Labarca, P. Charnet, N. Davidson, and H. A. Lester. 1988. Evidence that the M2 membrane-spanning region lines the ion channel pore of the nicotinic receptor. *Science.* 242:1578–1581.

Lester, H. A. 1992. The permeation pathway of ligand-gated ion channels. *Annual Review of Biophysics and Biomolecular Structure.* 21:267–292.

Levitt, D. G. 1986. Interpretation of biological ion channel flux data-reaction-rate versus continuum theory. *Annual Review of Biophysics and Biophysical Chemistry.* 15:29–57.

Lo, D. C., J. L. Pinkham, and C. F. Stevens. 1990. Influence of the γ subunit and expression system on acetylcholine receptor gating. *Neuron.* 5:857–866.

Maeno, T., C. Edwards, and M. Anraku. 1977. Permeability of the endplate membrane activated by acetylcholine to some organic cations. *Journal of Neurobiology.* 8:173–184.

Miledi, R. 1982. A calcium-dependent transient outward current in *Xenopus laevis* oocytes. *Proceedings of the Royal Society of London, Series B.* 215:491–497.

Mishina, M., T. Kurosaki, T. Tobimatsu, Y. Morimoto, M. Noda, T. Yamamoto, M. Terao, J. Lindstrom, T. Takahashi, M. Kuno, and S. Numa. 1984. Expression of functional acetylcholine receptor from cloned cDNAs. *Nature.* 307:604–608.

Mishina, M., T. Tobimatsu, K. Imoto, K. I. Tanaka, Y. Fujita, K. Fukuda, M. Kurasaki, H. Takahashi, Y. Morimoto, T. Hirose et al. 1985. Localization of functional regions of acetylcholine receptor α-subunit by site-directed mutagenesis. *Nature.* 313:364–369.

Noda, M., H. Takahashi, T. Tanabe, M. Toyosato, Y. Furutani, T. Hirose, M. Asai, S. Inayama, T. Miyata, and S. Numa. 1982. Primary structure of α-subunit precursor of *Torpedo californica* acetylcholine receptor deduced from cDNA sequence. *Nature.* 299:793–797.

Noda, M., H. Takahashi, T. Tanabe, M. Toyosato, S. Kikyotani, T. Hirose, M. Asai, H. Takashima, S.

Inayama, T. Miyata, and S. Numa. 1983. Primary structures of β and δ subunit precursors of *Torpedo californica* acetylcholine receptor deduced from cDNA sequences. *Nature.* 301:251–255.

Oberthür, W., P. Muhn, H. Baumann, F. Lottspeich, B. Wittmann-Liebold, and F. Hucho. 1986. The reaction site of a non-competitive antagonist in the γ-subunit of the nicotinic acetylcholine receptor. *EMBO Journal.* 5:1815–1819.

Oiki, S., W. Dahno, V. Madison, and M. Montal. 1988. M2 δ, a candidate for the structure lining the ionic channel of the nicotinic cholinergic receptor. *Proceedings of the National Academy of Sciences, USA.* 85:8703–8707.

Oiki, S., V. Madison, and M. Montal. 1990. Bundles of amphipathic transmembrane α-helices as a structural motif for ion-conducting channel proteins: studies on sodium channels and acetylcholine receptors. *Proteins: Structure, Function, and Genetics.* 8:226–236.

Okamoto, T., and K. Sumikawa. 1991. Antibiotics cause changes in the desensitization of ACh receptors expressed in *Xenopus* oocytes. *Molecular Brain Research.* 9:165–168.

Pauling, L., R. B. Corey, and H. R. Branson. 1951. The structure of proteins: two hydrogen-bonded helical configurations of the polypeptide chain. *Proceedings of the National Academy of Sciences, USA.* 37:205–211.

Revah, F., J. Galzi, J. Giraudat, P. Haumont, F. Lederer, and J. P. Changeux. 1990. The non-competitive blocker [^{3}H]chlorpromazine labels three amino acids of the acetylcholine receptor γ subunit: implications for the α-helical organization of regions MII and for the structure of the ion channel. *Proceedings of the National Academy of Sciences, USA.* 87:4675–4679.

Ritchie, A. K., and D. M. Fambrough. 1975. Ionic properties of the acetylcholine receptor in cultured rat myotubes. *Journal of General Physiology.* 65:751–767.

Sakmann, B., C. Methfessel, M. Mishina, T. Takahashi, T. Takai, M. Kurasaki, K. Fukuda, K., and S. Numa. 1985. Role of acetylcholine receptor subunits in gating of the channel. *Nature.* 318:538–543.

Sanchez, J. A., J. A. Dani, D. Siemen, and B. Hille. 1986. Slow permeation of organic cations in acetylcholine receptor channels. *Journal of General Physiology.* 87:985–1001.

Stroud, R. M., M. P. McCarthy, and M. Shuster. 1990. Nicotinic acetylcholine receptor superfamily of ligand-gated ion channels. *Biochemistry.* 29:11009–11023.

Trautmann, A., and N. F. Zilber-Gachelin. 1976. Further investigations on the effect of denervation and pH on the conductance change at the neuromuscular junction of the frog. *Pflügers Archiv.* 364:53–58.

Villarroel, A., S. Herlitze, M. Koenen, and B. Sakmann. 1991. Location of a threonine residue in the α-subunit M2 transmembrane segment that determines the ion flow through the acetylcholine receptor channel. *Proceedings of the Royal Society of London, Series B.* 243:69–74.

White, M. M. 1987. "Deltaless" acetylcholine receptors are highly voltage-dependent. *Society for Neuroscience Abstracts.* 13:798.

White, M. M., and M. Aylwin. 1990. Niflumic and flufenamic acids are potent blockers of Ca^{2+}-activated Cl^- channels in *Xenopus* oocytes. *Molecular Pharmacology.* 37:720–724.

White, M. M., K. Mixter-Mayne, H. A. Lester, and N. Davidson. 1985. Mouse-Torpedo hybrid acetylcholine receptors: functional homology does not equal sequence homology. *Proceedings of the National Academy of Sciences, USA.* 82:4852–4856.

Yoshii, K., L. Yu, K. Mixter-Mayne, N. Davidson, and H. A. Lester. 1987. Equilibrium properties of mouse-Torpedo acetylcholine receptor hybrids expressed in *Xenopus* oocytes. *Journal of General Physiology.* 90:553–573.

Yu, L., R. J. LaPolla, and N. Davidson. 1986. Mouse muscle nicotinic acetylcholine receptor γ subunit: cDNA sequence and gene expression. *Nucleic Acids Research.* 14:3539–3555.

Zar, J. H. 1984. Biostatistical Analysis. Prentice-Hall, Englewood Cliffs, NJ. 186–190.